

Final Technical Report

***Nano-Scale Interpenetrating Phase
Composites (IPC'S) for Industrial and
Vehicle Applications***

April 2010

Principal Investigators:

Dr. J. G. Hemrick
Dr. M. Z. Hu
Oak Ridge National Laboratory

Klaus-Markus Peters
Fireline TCON, Inc.

Brian Hetzel
Fireline, Inc.



Managed by UT-Battelle, LLC

ORNL/TM-2010/80

DOCUMENT AVAILABILITY

Reports produced after January 1, 1996, are generally available free via the U.S. Department of Energy (DOE) Information Bridge.

Web site <http://www.osti.gov/bridge>

Reports produced before January 1, 1996, may be purchased by members of the public from the following source.

National Technical Information Service
5285 Port Royal Road
Springfield, VA 22161
Telephone 703-605-6000 (1-800-553-6847)
TDD 703-487-4639
Fax 703-605-6900
E-mail info@ntis.fedworld.gov
Web site <http://www.ntis.gov/support/ordernowabout.htm>

Reports are available to DOE employees, DOE contractors, Energy Technology Data Exchange (ETDE) representatives, and International Nuclear Information System (INIS) representatives from the following source.

Office of Scientific and Technical Information
P.O. Box 62
Oak Ridge, TN 37831
Telephone 865-576-8401
Fax 865-576-5728
E-mail reports@adonis.osti.gov
Web site <http://www.osti.gov/contact.html>

FINAL TECHNICAL REPORT

Project Title: Nano-Scale Interpenetrating Phase Composites (IPC'S) for Industrial and Vehicle Applications

Project Period: October 2008 – September 2009

PI(s): Dr. J.G. Hemrick
(865) 776-0758
hemrickjg@ornl.gov

Dr. M.Z Hu
(865) 574-8782
hum1@ornl.gov

Recipient: Oak Ridge National Laboratory (ORNL)
Bethel Valley Road
P.O. Box 2008
Oak Ridge, TN 37831

Subcontractor: Oak Ridge National Laboratory (ORNL)
Bethel Valley Road
P.O. Box 2008
Oak Ridge, TN 37831

Nano-Scale Interpenetrating Phase Composites (IPC'S) for Industrial and Vehicle Applications

James G. Hemrick¹, Michael Hu², Klaus-Markus Peters³, and Brian Hetzel⁴

April 2010

Prepared by
OAK RIDGE NATIONAL LABORATORY
P.O. Box 2008
Oak Ridge, Tennessee 37831-6283
managed by
UT-Battelle, LLC
for the
U.S. DEPARTMENT OF ENERGY
under contract DE-AC05-00OR22725

¹ Oak Ridge National Laboratory, Material Science and Technology Division, Oak Ridge, TN

² Oak Ridge National Laboratory, Nuclear Science and Technology Division, Oak Ridge, TN

³ Fireline TCON, Inc., Youngstown, OH

⁴ Fireline, Inc., Youngstown, OH

Table of Contents

List of Tables and Figures.....	v
Abbreviations and Acronyms.....	vii
1. Executive Summary.....	1
2. Introduction.....	5
2.1 Technical Objectives and Potential Markets.....	5
2.2 Potential Energy, Environmental, and Economic Benefits.....	7
3. Background.....	11
4. Project Technical Objectives.....	12
5. Tasks and Results.....	14
5.1 Investigation of Low Temperature Processes for Nano-Scale IPC Production.....	14
5.2 Investigation of High Temperature Processes for Nano-Scale IPC Production.....	18
5.3 Project Milestones.....	29
5.4 Lux Research Activities.....	29
6. Summary.....	30
7. Suggested Follow-On Activities.....	32
8. Acknowledgements.....	34
9. References.....	35
10. Distribution.....	39

List of Tables and Figures

Tables

Table 1. U.S. Industry Energy Analysis.....	7
Table 2. Energy Metrics from Industrial GPRA Analysis.....	8
Table 3. Environmental Metrics from Industrial GPRA Analysis.....	8
Table 4. Energy Metrics from Vehicle GPRA Analysis.....	10
Table 5. Environmental Metrics from Vehicle GPRA Analysis.....	10
Table 6. Financial Metrics from Industrial GPRA Analysis.....	10
Table 7. Financial Metrics from Vehicle GPRA Analysis.....	11
Table 8. Matrix for TCON Sample Preparation.....	20
Table 9. TCON Flexure Strength Values.....	22

Figures

Figure 1. Fuel savings (a) and greenhouse gas emissions reductions (b) from hypothetical fuel economy improvements.....	9
Figure 2. TEM bright-field image (a) and high resolution TEM image (b) of a copper (Cu)/alumina (Al ₂ O ₃) IPC nanocomposite.....	12
Figure 3. General microstructure of current Fireline TCON IPC materials showing alumina ceramic phase and aluminum metal phase (a) and reduced-scale microstructure of experimental Fireline TCON IPC material showing alumina ceramic phase with aluminum metal phase and intermetallic (IMC) phase due to metallic iron addition (b).....	13
Figure 4. Example of controlled diffusion/evaporation during sol-gel and block-copolymer template synthesis. (A) Initial liquid solution that contains mix of sol-gel inorganic precursors and block-copolymer template molecules. (B) A monolithic solid matrix is forming during liquid-to-solid transformation processing. (C) A completely formed dry solid matrix inside the molding reactor. (D) A free standing solid monolithic matrix that contains desirable interpenetrating, open nanopores.....	15
Figure 5. STEM images of nanopore (7.5 nm) nanostructures inside specimens on a TEM grid, prepared by block-copolymer template sol-gel synthesis. (a) lamellar microphase (b) mixed phase (c) hexagonal phase. Note: darker lines or dots correspond to nanopores, and the bright lines correspond to the inorganic (silica) matrix.....	16
Figure 6. Nanopore channels in anodized aluminum oxide (AAO) and anodized Titanium oxide (ATO).....	17
Figure 7. Schematic of bi-continuous phase structure.....	18
Figure 8. Examples of PNNL mesoporous and nanoporous substrate production showing a mesoporous silica microstructure (a) and a route to a nanoporous ceramic substrate (b).....	19
Figure 9. Pictures of prepared experimental TCON samples from Run #1 (a), #2 (b), #3 (c), #4 (d), #5 (e), #6 (f), #7 (g), #8 (h), and #9 (i).....	21
Figure 10. TCON flexure strength vs. sample run and processing conditions.....	22

Figure 11. Optical microscopy of clay preform (Run #8) sample cross section exhibiting large porosity of transformed sample	24
Figure 12. TEM images of Run #2 sample (fused quartz/Al-25%Si alloy/24 hour transformation time).....	25
Figure 13. SEM (a) and TEM (b) images of Run #4 sample (fused quartz/Al-7.5%Fe alloy/4.63 hour transformation time).....	26
Figure 14. TEM image of Run #5 sample (fused quartz/Al-3% Ti alloy/4.83 hour transformation time).....	27
Figure 15. TEM images of Run #6 sample (fused quartz/Al-2.5%Mg alloy/23.5 hour transformation time).....	27
Figure 16. TEM image of Run #7 sample (Vycor™ glass/pure Al /2 hour transformation time).....	28
Figure 17. TEM images of Run #8 sample (clay/pure Al /8 hour transformation time).....	29

Abbreviations and Acronyms

AAO	Anodized Aluminum Oxide
Al	Aluminum
Al ₂ O ₃	Alumina
ATO	Anodized Titanium Oxide
bcf	billion cubic feet
BES	Basic Energy Sciences
CAFÉ	Corporate Average Fuel Economy
CICM	Co-continuous Interpenetrating Ceramic-Metal
CO	Carbon Monoxide
Cu	Copper
DOD	U.S. Department of Defense
DOE	U.S. Department of Energy
FIB	Focused Ion Beam
Fe	Iron
FTA	Federal Transit Administration
GPRA	Government Performance and Reporting Act
hr.	hour
IMC	Intermetallic Compound
IPC	Interpenetrating Phase Composite
ksi	kilo-pound per square inch
Mg	Magnesium
mm	millimeter
MPa	Mega Pascal
MPG	Miles per Gallon
nm	nanometer
NO _x	Nitrous Oxides
ORNL	Oak Ridge National Laboratory
PNNL	Pacific Northwest National Laboratory
RMP	Reactive Metal Penetration
SEM	Scanning Electron Microscopy
SEM/EDS	Scanning Electron Microscopy/Energy Dispersive Spectroscopy
Si	Silicon
SiO ₂	Silica
STEM	Scanning Transmission Electron Microscope
T	Temperature
TBtu	Trillion BTU (British Thermal Units)
TEM	Transmission Electron Microscope
Ti	Titanium
VOC	Volatile Organic Compound
vs.	verses
yr.	year
YSU	Youngstown State University

1. Executive Summary

A one-year project was completed at Oak Ridge National Laboratory (ORNL) to explore the technical and economic feasibility of producing nano-scale Interpenetrating Phase Composite (IPC) components of a usable size for actual testing/implementation in real applications such as high wear/corrosion resistant refractory shapes for industrial applications, lightweight vehicle braking system components, or lower cost/higher performance military body and vehicle armor. Nano-scale IPC's with improved mechanical, electrical, and thermal properties have previously been demonstrated at the lab scale, but have been limited in size. The work performed under this project was focused on investigating the ability to take the current traditional lab scale processes to a manufacturing scale through scaling of these processes or through the utilization of an alternative high-temperature process.

IPC's are defined as multiphase composites in which each phase is topologically interconnected throughout the microstructure. Materials such as these are commonly found in nature in structures like bones, plant limbs, and tree trunks and were of interest to DOE Basic Energy Sciences (DOE-BES) as far back as 1989. Unique properties can be realized in this class of materials due to their three-dimensional microstructure which leads to multifunctional characteristics dictated by each continuous individual component.

IPC materials can be fabricated in-situ through processes such as spinodal decomposition (a mechanism by which a solution of two components can separate into distinct regions or phases with distinctly different chemical compositions and physical properties such as what occurs in Vycor™ glasses), by infiltration of a porous solid preform followed by consolidation (the low temperature process investigated in this work), or through chemical reactions (the high temperature process investigated in this work). Each of these processes will affect the resulting material's microstructure, which has been shown to influence both its mechanical and physical characteristics. When the microstructure is on the nano-scale level, property manipulation seems to be even more significant. Therefore, nano-scale IPC's are of interest where the co-continuous interconnected phases each yield unique properties due to their nanostructure and combine to produce a bulk material with optimized performance and multifunctional characteristics.

Significant energy savings and environmental benefits were estimated to be possible through this project through utilization of IPC materials in two areas. The first was possible savings and benefits due to application in industrial sectors such as the aluminum, copper, glass, iron & steel, metal casting, and super alloy industries. Possible energy savings and environmental benefits were calculated using the DOE GPR (Government Performance and Reporting Act) spreadsheet resulting in total primary energy that could be displaced by the year 2030 estimated at 20 TBtu/yr. and the direct natural gas that could be displaced annually at nearly 20 bcf/yr. The associated estimated environmental benefit to using IPC materials in industrial applications was estimated at 580 metric tons of CO that could be displaced, 2,143 metric tons of NO_x that could be displaced, and 54.5 metric tons of VOC's that could be displaced by the year 2030.

The second area analyzed was benefits due to application of IPC materials in vehicle applications. Using plots from CAFÉ Standards released by the Transportation Research Board, a reduction in fuel consumption and greenhouse gas emissions was estimated based on a 5% increase in MPG (resulting from a 3-5% decrease in vehicle weight) by year 2030 resulting in an approximate savings of 7,000 million gallons of fuel per year and an approximate reduction in greenhouse gas emissions of 20 million metric tons carbon equivalent per year. Possible energy savings and environmental benefits were also calculated using the DOE GPRA spreadsheet and the assumptions above. A 5% improvement in fuel economy was predicted to reduce oil consumption to 2,774 million barrels a year resulting in the total direct petroleum displaced by the year 2030 estimated at 0.50 million barrels a year. Even larger impact was predicted to be possible with expanded implementation of the technology. Additionally, environmental benefits possible when using IPC materials in vehicle applications were estimated at 580 metric tons of CO displaced, 2143 metric tons of NO_x displaced, and 54.5 metric tons of VOC's displaced by the year 2030.

One part of the project looked at the traditional low temperature process for producing nano-scale IPC materials and focused on identifying ways to improve the infiltration and wetting of metal into the nanoporous ceramic substrate to decrease the porosity and increase the performance. Such concepts as room temperature electroless infiltration processing to determine optimized methods for infiltration of metal into ceramic substrates, preparation of a nanoporous ceramic matrices (nano-foams), low temperature electrochemical infiltration, and low-temperature routes to create co-continuous interpenetrating ceramic-metal (CICM) nano-composites were pursued.

A second part of the project investigated the use of an alternative high temperature process for IPC production and focused on reduction of the current length scale of materials produced by this process from the micro- to the nano-scale. Such concepts as the introduction of metallic additions were investigated along with changes in preform choice and alteration of processing conditions. Control of reaction rates and their effect on size scale of the structure were also considered, as well as the competition between active mechanisms in the process (acceleration due to conditions or additives, wetting behavior and penetration rates due to additives). Samples incorporating metallic additions were made through the use of metal alloys obtained as master alloys (Al-Si, Al-Fe, Al-Ti, and Al-Mg). Alternative preforms were identified and samples were prepared using fused quartz, Vycor™ glass and clay. The detailed mechanisms of the transformation process (mass transfer rate, diffusion, and reaction kinetics) were also investigated.

It was determined that it appears improved nano-scale IPC materials can be produced through identified improved low temperature metal infiltration and wetting techniques as well as through the use of the alternative high temperature process with the use of select metallic additions to produce intermetallic compound (IMC) or solid solution phases. Additionally, size scaling of materials produced by the improved low temperature methods is believed to be possible based on preliminary results achieved at ORNL and through the use of alternative preform materials, the high temperature process may result

in a reduction of the length scale of TCON materials from the micro-scale to the nano-scale.

One identified route for production of IPC materials by low temperature methods was the infiltration of metal into a nanoporous ceramic matrix. It was determined that the greatest challenges to such a method included: (1) the creation of a nanoporous ceramic matrix containing open, interconnected nanopores (1-100 nm), or simply called ceramic “nano-foam” and (2) the actual penetration of metal into the nanopores. Regarding the preparation of the nanoporous ceramic matrix, anodized aluminum oxide containing parallel channel pores was investigated which can serve as a model system for study of infiltration and property measurements. Regarding low temperature electrochemical infiltration, a method was demonstrated at ORNL to deposit and accumulate a metallic phase into the nanopores of a ceramic substrate. This method improves upon the traditional method for fabrication of porous ceramic materials by ceramic powder pressing and sintering, which has the limitation of not being able to create uniform, interconnected, open pores of nanometer scale.

Low-temperature routes to create CICM nano-composites were also evaluated. The focus was on the conceptual development of three promising routes: 1) low temperature co-sintering of mixed ceramic and metallic nanopowders, 2) infiltration of metal into nanoporous cellular ceramics or ceramic nano-foams, and 3) co-formation of bi-continuous block copolymer microphases with ceramic and metal precursors.

Actual samples, some exhibiting nano-scale and increased strengths, were prepared using the alternative high temperature process incorporating various metallic additions, alternative preform materials, and varying processing times. Samples produced with Al-Fe alloy in place of pure Al showed a considerable increase in flexure strength due to the formation of a nano-featured intermetallic compound (IMC) phase and materials with Al-Mg alloy in place of pure Al resulted in an IPC with a nanostructured solid solution phase and greatly increased flexure strength. Yet, through analysis of flexure strength values and microstructure it was determined that transformation time did not appear to affect the microstructure in a manner that affected the strength of the resulting material. Further, the addition of Al-Si alloy in place of pure Al resulted in materials with only slightly higher strength than standard material.

Material which was produced using Al-Ti in place of pure Al was found to be weaker in flexure strength than the other materials incorporating metallic additions, but still slightly stronger than standard material, as the resulting material did not reveal the expected Al-Ti intermetallic phase that was hoped to be formed leading to increased strength. Material produced using a Vycor™ glass preform in place of fused quartz was found to show a flexure strength similar to that of materials produced using fused quartz preforms processed with Al-Si alloy and materials produced using fused quartz preforms processed with Al-Ti alloy. The flexure strength of this material was only slightly higher than that of standard material, indicating that the use of Vycor™ glass preforms instead of fused quartz may lead to only slightly increased strengths. Material produced using a clay preform material in place of fused quartz showed a difficulty in fully transforming. This

resulted in a large degree of porosity in the final IPC creating a relatively open structure in these materials which is expected to have led to the decrease in the mechanical properties exhibited through the low measured flexure strength and relatively high variability among test pieces.

2. Introduction

2.1 Technical Objectives and Potential Markets

This one-year project at Oak Ridge National Laboratory (ORNL) proposed to explore the technical and economic feasibility of producing nano-scale Interpenetrating Phase Composite (IPC) components of a usable size for actual testing/implementation in a real applications such as high wear/corrosion resistant refractory shapes for industrial applications, lightweight vehicle braking system components, or lower cost/higher performance military body and vehicle armor. Nano-scale IPC's with improved mechanical, electrical, and thermal properties have previously been demonstrated at the lab scale (both in the literature and at ORNL), but have been limited to thin films. The work performed under this project was focused on investigating the ability to take the current traditional lab scale processes to a manufacturing scale through improvement and scaling of the current processes or utilization of an alternative process.

Although IPC nanomaterials with unique properties have been produced in the lab, components of useable size for actual application have not been possible with the current processes. This has been partly due to difficulties in infiltrating the preform due to low wetting between the metal and ceramic phases and inability to fill closed pores within the preform leading to inhomogeneity in the nanostructure of the infiltrated materials and a reduction of desired performance. Additionally, there has not been an effort made to scale up these processes to produce large components of a suitable size for use in actual applications

The first part of the project investigated methods to improve and scale up the current common low temperature processing techniques used to produce nano-scale IPC's and evaluated the technical and economic feasibility of such a scale up. The second part of this project evaluated the modification of an alternative high temperature commercial process (developed and used by Fireline TCON, Inc.) for producing component sized micro-scale (≈ 100 nm microstructures) IPC materials through displacement reactions. Actual industrial sized components have been produced by this method and shown to be effective for use in molten metal contact applications where increased abrasion/wear resistance and corrosion resistance are required^{1,2}. The current investigation explored the technical and economic feasibility of modifying the process to produce nano-scale IPC components with the intent that reduction in the structures of these materials from the micro- to the nano-scale would lead to improvements in the mechanical, electrical, and thermal properties of these components resulting in further energy and economic benefits due to their use. The hope was that if either or both of these approaches proved viable, a path for producing useable nanocomposite-based functional materials for industrial and automotive applications would be realized for further development and commercialization.

The first market targeted for impact by nano-scale IPC's with improved mechanical and thermal properties was the industrial molten metal/glass containment and insulation market. Most industrial processes (the aluminum, copper, glass, iron & steel, metal casting, and super alloy industries for example) utilize high temperature process vessels which require refractory linings³. Energy efficiency of these high temperature industrial

processes is limited by the ability of the materials to resist mechanical degradation (abrasion and wear), corrosion by the service environments, and deterioration due to thermal cycling or shock. Additionally, these materials are often called upon to also provide insulation to the process and to keep process heat in the service load. As these materials degrade, the ability to do this is decreased exponentially and the need to maintain or replace the materials is created. Such maintenance often requires cooling of the furnace or refractory lined vessel which entails loss of energy due to cooling and consumption of energy due to reheating. Finally, a loss in production time and capability is sacrificed.

The second market targeted for impact by nano-scale IPC's with improved mechanical and thermal properties is the vehicle industry. One way to reduce vehicle weight and therefore increase fuel efficiency is through the development of lightweight components for advanced braking systems. Additionally lighter weight material systems for automotive applications are sought to make electric and fuel cell vehicles possible. As stated in the Federal Transit Administration's (FTA) *Strategic Research Plan*, September 30, 2005: "Researching technologies to reduce vehicle weight can also lead to important reductions in fuel consumption and emissions. The power required to accelerate a bus and overcome rolling resistance is directly proportional to vehicle weight. Composite materials are one example of an FTA research area aimed at reducing vehicle weights." Also, longer life components will reduce the frequency of replacing these parts, leading to a reduction in manufacturing costs and energy to produce additional replacement parts. For example, estimates show that a reduction of vehicle weight of only 5% will result in a fuel economy improvement of 3-4%⁴.

For the personal and commercial vehicle industries, gray cast iron has been the overwhelming material of choice in braking systems (such as in brake rotors and drums) because it is inexpensive and a large supply chain infrastructure is in place for engineering and manufacturing gray cast iron components. However, gray cast iron is a relatively heavy material. Utilizing lighter weight materials in braking systems would not only achieve better fuel economy by reducing the vehicle's static weight but, since brake rotors and drums are rotating components, there would be a large multiplying effect on reducing the amount of energy required to increase their rotational speed as the vehicle accelerates. Finally, as the braking system is an unsprung weight, a lighter system would significantly improve vehicle handling performance and safety. Most lightweight materials do not have the physical, mechanical, thermal, and tribological performance characteristics required for brake applications, such as a high strength and high thermal conductivity at elevated temperatures. Lightweight alternatives to gray cast iron that currently do exist are prohibitively expensive for general use in most vehicles⁵. Initial research on next-generation materials for brake rotors has already evaluated composites similar to TCON materials (i.e., IPC's produced via reactive metal penetration (RMP) processes). The preliminary results were very promising, showing that these IPC's exhibited friction and wear properties similar to cast iron, but with half the weight and better thermal conductivity⁶. It is thought that nano-scaled IPC components could show further improvements in mechanical, electrical, and thermal properties leading to even better performance in this application.

Finally, the materials developed under this project could be utilized for lower cost/higher performance military body and vehicle armor applications. Ceramic-based armor (based on SiC) has been shown to weigh 55% less than identically sized steel plate armor and armor based on nanoparticles (carbon nanotubes) is hypothesized to be 100 times stronger and weigh 83% less than equivalent steel-based armor. Therefore there is great interest in the development of cost-efficient scalable production methods for nano-scaled materials which may find use in armor applications⁷. The TCON materials under investigation in this proposal are composites of alumina and silicon carbide, two materials considered in the past for incorporation into force protection packages. Although this was out of the scope of the original DOE call to which this project was a response (larger efforts are underway by Department of Defense (DOD) and Homeland Security), such reductions in armor weight could result in reduced personnel weight in military vehicles and reduced weight of armor used on vehicles (helicopters, aircraft, Humvees, and personnel carriers), both of which will lead to reduced fuel consumption. The successful commercialization of such newly developed force protection materials could also be leveraged into the non-military markets, such as for police and fire fighting forces.

2.2 Potential Energy, Environmental, and Economic Benefits

Energy savings and environmental benefits were calculated in two steps. The first looked at possible savings and benefits due to application of IPC materials in industrial applications such as the aluminum, copper, glass, iron & steel, metal casting, and super alloy industries. For this analysis, the total energy usage for the U.S. aluminum, fabricated metals, foundry, and glass industries were considered as shown in Table 1. Additionally, the estimated percent total energy affected by refractory materials (insulation and containment materials) for each industry is shown and the resulting energy value affected. Finally, assuming a conservative improvement of 2% and an aggressive improvement of 10%, possible energy savings for each industry are shown.

Table 1. U.S. Industry Energy Analysis

Industry	NAICS codes	Total TBtu/year ^a	Usage affected by refractories		Energy savings goals for improved refractories (TBtu/Yr)	
			%	TBtu/Yr	Near-term 2%	Long-term 10%
Aluminum	3313XX1	441	90%	397	7.9	39.7
Fabricated Metals	33281	445	90%	401	8.0	40.1
Foundries	3315XX	233	90%	210	4.2	21.0
Glass	3272XX	203	70%	142	2.8	14.2

^a TBtu = trillion Btu/year. *Source:* U.S. Department of Energy, Energy Information Administration, 1998 *MECS Consumption*, Table N3.2, Fuel Consumption, 1998.

(from energy calculations performed during writing of “Refractories for Industrial Processing: Opportunities for Improved Energy Efficiency” by Hemrick et. al., values published in same report³)

Possible energy savings and environmental benefits were then calculated using the DOE GPRA (Government Performance and Reporting Act) spreadsheet and the values above. To perform the analysis, the effects of refractory improvement were estimated by summing the total energy usage (natural gas consumption) for each industry affected by refractories as shown in Table 1. This resulted in a total of 1,150 TBtu/yr. (2.23 billion cubic feet of natural gas). Improvements due to new technology were estimated to account for a 5% improvement in energy efficiency. This value was between the near-term and long term energy savings goals shown in Table 1. The total number of units affected by the improved technology was chosen to be 500 representing 500 plants implementing the technology. Annual market growth rate was set at 1.0%, with an ultimate potential accessible market of 100% and likely technology market share of 30%.

As shown in Table 2, there is an appreciable estimated energy savings realized by implementing IPC materials in these industrial applications. The total primary energy that could be displaced by the year 2030 is estimated at 20 TBtu/yr. and the direct natural gas that could be displaced annually is nearly 20 bcf/yr. As shown in Table 3, there is also an estimated environmental benefit to using IPC materials in industrial applications with an estimated 580 metric tons of CO that could be displaced, 2,143 metric tons of NO_x that could be displaced, and 54.5 metric tons of VOC's that could be displaced by the year 2030.

Table 2. Energy Metrics from Industrial GPRA Analysis

	2015	2020	2025	2030
Total primary energy displaced annually (TBtu/yr.)	0.36	2.99	12.75	20.17
Cumulative total primary energy displaced (TBtu)	0.60	8.37	50.35	139.94
Direct natural gas displaced annually (bcf/yr.)	0.35	2.91	12.41	19.64
Cumulative direct natural gas displaced (bcf)	0.58	8.15	49.03	136.26

Table 3. Environmental Metrics from Industrial GPRA Analysis

	2015	2020	2025	2030
CO displaced annually (metric tonnes/yr.)	10.48	86.18	367.01	580.91
Cumulative CO displaced (metric tonnes)	17.21	241.13	1449.93	4029.45
NO _x displaced annually (metric tonnes/yr.)	38.67	317.98	1354.20	2143.46
Cumulative NO _x displaced (metric tonnes)	63.51	889.72	5349.95	14867.86
VOCs displaced annually (metric tonnes/yr.)	1.07	8.83	37.59	59.49
Cumulative VOCs displaced (metric tonnes)	1.76	24.69	148.49	412.67

The second step looked at possible savings and benefits due to application of IPC materials in vehicle applications. For this analysis, the assumption that a 5% reduction in vehicle weight will result in a 3-4% improvement in fuel efficiency was used as was estimated in the Transportation Research Board document Effectiveness and Impact of Corporate Average Fuel Economy (CAFE) Standards referenced above⁴. The corresponding reduction in fuel consumption and greenhouse gas emissions was first estimated using the two plots in Figure 1 (from the above document). Extrapolating from Figure 1(a) it is estimated that a 5% increase in MPG (resulting from a 3-5% decrease in vehicle weight) by year 2030 would result in an approximate savings of 7,000 million gallons of fuel per year and from Figure 1(b) an approximate reduction in greenhouse gas emissions of 20 million metric tons carbon equivalent per year (assuming 5% MPG increase would be roughly 1/3 the benefit of a 15% increase).

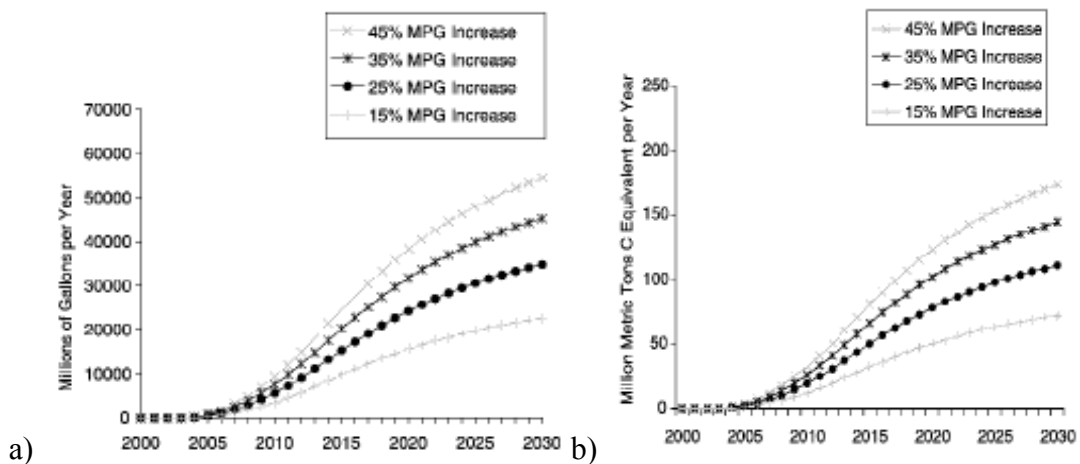


Figure 1. Fuel savings (a) and greenhouse gas emissions reductions (b) from hypothetical fuel economy improvements.⁴

Possible energy savings and environmental benefits were also calculated using the DOE GPRA spreadsheet and the assumption of a 3-5% reduction of vehicle weight leading to a 5% increase in fuel economy. According to the Environmental Protection Agency, September 2001 report “Light-Duty Automotive Technology and Fuel Economy Trends: 1975-2001”, cars, SUV’s and other light trucks in the U.S. consume an average of 8 million barrels of oil every day (2,920 million barrels of oil a year). Therefore, a 5% improvement in fuel economy would reduce this number to 2,774 million barrels of oil a year. The total number of units affected by the improved technology was chosen to be 12.5 million, representing 5% of the estimated 250 million automobiles⁸ in the U.S. implementing the technology. Annual market growth rate was set at 1.0%, with an ultimate potential accessible market of 100% and likely technology market share of 30%. As shown in Table 4, there is a measurable energy savings estimated by implementing IPC materials in vehicle applications when only making this small improvement with the total direct petroleum displaced by the year 2030 estimated at 0.50 million barrels a year. Even larger impact would be possible with expanded implementation.

Table 4. Energy Metrics from Vehicle GPRA Analysis

	2015	2020	2025	2030
Direct petroleum displaced annually (million barrels)	0.01	0.07	0.32	0.50
Cumulative direct petroleum displaced (million barrels)	0.01	0.21	1.26	3.50

As shown in Table 5, there are also environmental benefits possible when using IPC materials in vehicle applications. By implementing these materials, it is estimated that by the year 2030; 580 metric tons of CO could be displaced, 2143 metric tons of NO_x could be displaced, and 54.5 metric tons of VOC's could be displaced.

Table 5. Environmental Metrics from Vehicle GPRA Analysis

	2015	2020	2025	2030
CO displaced annually (metric tons/yr.)	0.76	6.26	26.65	42.18
Cumulative CO displaced (metric tons)	3.81	35.10	168.35	379.28
NO _x displaced annually (metric tonnes/yr)	7.98	65.65	279.59	442.53
Cumulative NO _x displaced (metric tons)	39.92	368.17	1766.10	3978.77
VOCs displaced annually (metric tons/yr.)	0.21	1.74	7.42	11.75
Cumulative VOCs displaced (metric tons)	1.06	9.77	46.89	105.63

Economic benefits due to implementation of IPC materials in both industrial and vehicle applications were also calculated using DOE GPRA spreadsheets as described above. Estimated economic benefits due to implementing IPC materials in industrial applications are shown in Table 6, while estimated economic benefits due to implementing IPC materials in vehicle applications are shown in Table 7.

Table 6. Financial Metrics from Industrial GPRA Analysis

	2015	2020	2025	2030
Net economic benefit annually (\$MM/yr.)	26.67	425.21	2583.77	7206.90
Cumulative net economic benefit (\$MM)	89.12	856.00	4132.99	9338.34
Energy cost savings (\$MM/yr.)	2.84	40.46	250.66	716.08
Cumulative energy cost savings (\$MM)	8.57	80.93	400.13	923.83

Table 7. Financial Metrics from Vehicle GPRA Analysis

	2015	2020	2025	2030
Energy cost savings (\$MM/yr.)	0.33	3.18	15.73	36.27
Cumulative energy cost savings (\$MM)	0.55	7.95	49.32	140.57

3. Background

Interpenetrating Phase Composites (IPC's) are defined as multiphase composites in which each phase is topologically interconnected throughout the microstructure⁹. Materials such as these are commonly found in nature in structures like bones, plant limbs, and tree trunks. These materials were of interest to DOE Basic Energy Sciences (DOE-BES) as far back as 1989 when they sponsored a workshop on the needs and opportunities which resulted in the basic review paper on these materials by Clarke with emphasis on processing approaches and properties⁹. Unique properties can be realized in this class of materials due to their three-dimensional microstructure which leads to multifunctional characteristics dictated by each continuous individual component.

IPC materials can be fabricated in-situ through processes such as spinodal decomposition (a mechanism by which a solution of two components can separate into distinct regions or phases with distinctly different chemical compositions and physical properties such as what occurs in Vycor™ glasses), by infiltration of a porous solid preform followed by consolidation (the low temperature process investigated in this work), or through chemical reactions (the high temperature process investigated in this work). Each of these fabrication routes often use preforms with interconnected porosity (micro- or nano-scale) produced by various means. Infiltration of the preform is generally performed by introduction of a molten metal though use of a vapor, liquid, or slurry and the mechanism of percolation¹⁰. This infiltration step can be followed by an oxidation step, as in the case of the materials produced by chemical reactions. Yet, as Clarke stated in 1992, “control of the processes so that composites having desired microstructural features and length scales can reproducibly be made is likely to be of central concern from a technical point of view”⁹.

A material's microstructure has been shown to influence both its mechanical and physical characteristics. When the microstructural features are on the nano-scale level, property manipulation can be even more significant. Therefore, nano-scale IPC's are of interest where the co-continuous interconnected phases each yield unique properties due to their nanostructure and combine to produce a bulk material with optimized performance and multifunctional characteristics.

Thin film lab-scale IPC's of nano-scale have been produced in the past which show increased mechanical, electrical, and thermal properties through alteration of microstructure, choice of preforms (composition and structural characteristics), introduction of additional elements, and choice of processing temperatures and times.¹¹⁻¹⁴ Current and previous work has used low or room temperature approaches such as electrochemical metal infiltration of a metal into a nanoporous ceramic substrate¹⁵ or

electroless infiltration of a metal into a compaction of nanostructured ceramic powders¹⁶ to produce nano-scaled IPC's. Transmission Electron Microscope (TEM) images of an example IPC produced by these methods are shown in Figure 2. Yet, these methods are limited by difficulties in infiltrating the preform due to low wetting between the metal and ceramic phases and inability to fill closed pores within the preform¹⁷. These issues have led to inhomogeneity in the nanostructure of the infiltrated materials and a reduction of desired performance. Furthermore, the success of applying the infiltration method to produce solid IPC's of bulk dimension containing nanostructures has yet to be demonstrated.

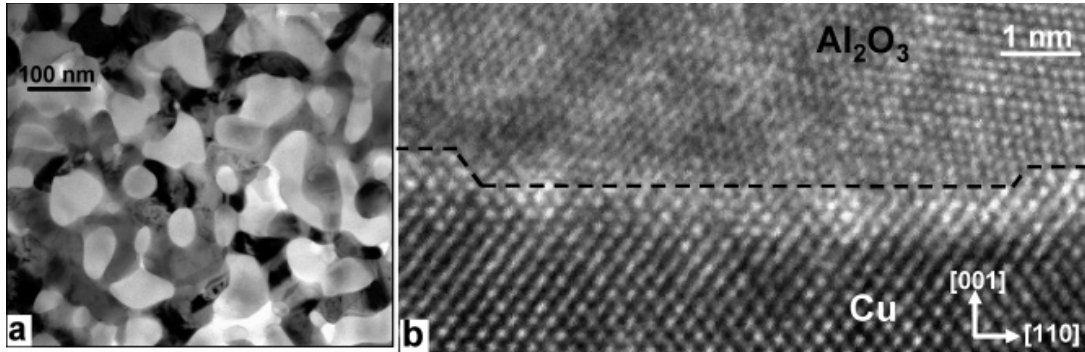
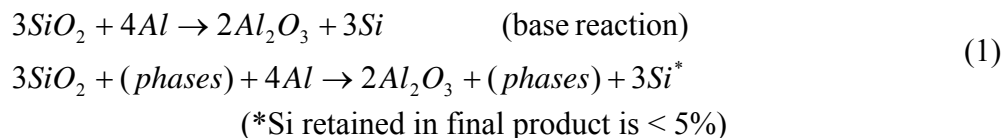


Figure 2. TEM bright-field image (a) and high resolution TEM image (b) of a copper (Cu)/alumina (Al_2O_3) IPC nanocomposite.¹⁵

4. Project Technical Objectives

One part of this project looked at the traditional low temperature process for producing nano-scale IPC materials and focused on identifying ways to improve the infiltration and wetting of metal into the nanoporous ceramic substrate to decrease the porosity and increase the performance. Such concepts as self-organized nanoporous ceramics and room-temperature electroless infiltration processes were investigated at ORNL. The mechanism of invasion percolation, with emphasis on the character of the infiltrant and the preform during the process, was considered, along with exploration of the process controls (optimization of current and bath) used to perform the infiltration. Choice of preform particle size and sintering conditions were also investigated. Ultimately, the technical and economic feasibilities of scaling the production of these materials from the lab-scale to a commercial scale were sought. Such ideas as volume scale up and multiplicative techniques in a series of electrochemical baths were considered to accomplish this.

Alternatively, the TCON[®] materials produced by Fireline (Youngstown, OH) are a class of IPC's produced by a unique reactive metal penetration (RMP) process as represented by Equation 1.



The process of transforming the preform into a TCON component is efficient, in that there are minimal dimensional changes; the part's shape and size are essentially

unchanged as the silica is converted to the alumina-aluminum alloy composite. Also, other materials can be added to the composite in order to tailor the final properties, such as silicon carbide particles for increased wear and thermal shock resistance.

These materials contain microscopic networks of ceramic and metallic phases that are co-continuous and strongly bonded together. This unique material structure is substantially different from traditional metal matrix and ceramic matrix composites, therefore TCON materials exhibit mechanical, physical and thermal properties that are quite distinctive. The presence of metallic phases provides significant improvement in toughness and damage tolerance, while the ceramic phases lead to high hardness and improved performance at elevated temperatures. Through current process variations, the properties of TCON composites can be tailored to meet the requirements of specific applications. TCON materials can be net-shaped or near-net shaped in a wide variety of useful forms and sizes, making the process relatively low cost. The current microstructure of these materials ranges from ≈ 100 nm to several microns as shown in Figure 3 (a). Yet, through preliminary work, it was postulated that metallic (Fe, Cu, Ti, Mg, etc.) additions to the microstructure may lead to further reduction to the nanostructure size range through the formation of intermetallic compound (IMC) phases (iron carbide in this case) as shown in Figure 3 (b).

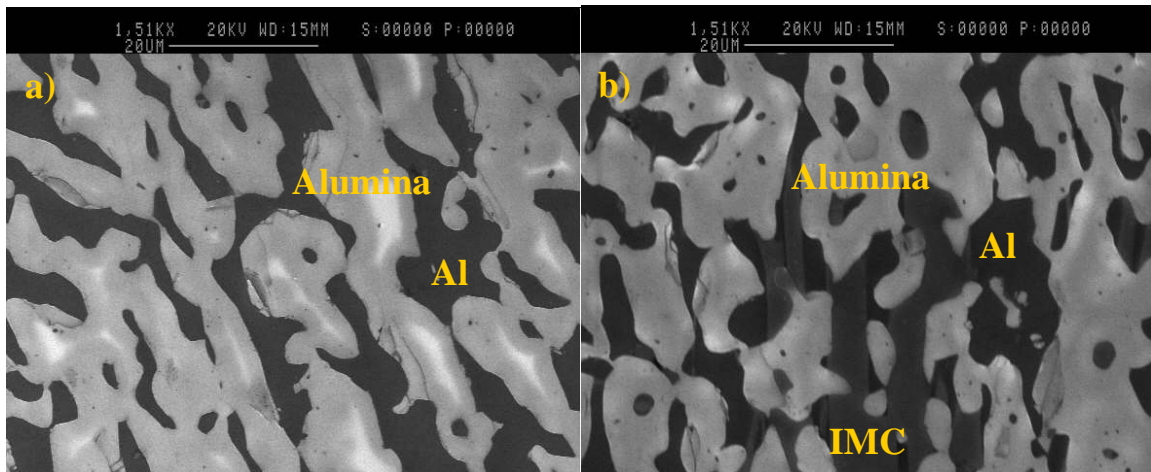


Figure 3. General microstructure of current Fireline TCON IPC materials showing alumina ceramic phase and aluminum metal phase (a) and reduced-scale microstructure of experimental Fireline TCON IPC material showing alumina ceramic phase with aluminum metal phase and intermetallic compound (IMC) phase due to metallic iron addition (b) as confirmed by SEM/EDS.

A second part of the project investigated this alternative high temperature process for IPC production and focused on reduction of the current length scale of materials produced by this process from the micro- to the nano-scale. Such concepts as the introduction of metallic additions mentioned above were investigated along with changes in preform choice and alteration of processing conditions. Control of reaction rates and their effect on size scale of the structure were also considered, as well as the competition between active mechanisms in the process (acceleration due to conditions or additives, wetting behavior and penetration rates due to additives). Previous work, for instance, has shown

that the addition of magnesium to molten aluminum enhances the penetration rate, while the process speed decreases with increases in preform porosity¹⁸. On the other hand, the addition of silicon decreases the infiltration rate but is needed in order to avoid the detrimental formation of aluminum carbide which embrittles the structure of the final part¹⁸.

One concern for using these materials at high temperatures, like those possible in industrial or vehicle applications, is grain coarsening and growth. It is thought that some resistance to such growth is provided by the mutual topological constraint of the constituent phases present in the IPC structure and by the morphology of the individual phases corresponding to minimal energy surfaces. This is supported by work in which experiments were performed on an IPC 50/50 mixture of alumina and zirconia and on single-phase alumina and zirconia samples. This work showed grain growth in the IPC was severely reduced compared to that seen in both single-phase materials¹⁹.

5. Tasks and Results

5.1 Investigation of Low Temperature Processes for Nano-Scale IPC Production

The following work was performed to determine the technical and economic feasibility of producing nano-scale IPC components of a useable size by traditional low temperature methods. Literature surveys were initially conducted on both IPC and nano-scale IPC materials produced by traditional low temperature methods. Results of this survey showed that there are limited publications on nano-scale IPC's. Justifications for considering the concept of nano-scale IPC's were then developed based on the potential benefits of: (1) the interpenetrating continuous phases and the nanostructure could improve the properties of metal-ceramic composites and (2) the continuous phases could allow the tailoring of properties by fully taking advantage of the properties of both phases. Additionally, a need was identified to continue development of the knowledge database for various categories of final applications so that answers to fundamental questions such as how the properties of nano-IPCs are improved over traditional IPC materials could be determined.

Initial experimental work was focused on investigation of the room temperature electroless infiltration processes to determine optimized methods for infiltration of metal into a ceramic substrate. One identified route was the infiltration of metal (such as Cu, Al, or an alloy) into a nanoporous ceramic matrix (such as alumina, silica, or titania). It was determined that the greatest challenges to such a method included: (1) the creation of a nanoporous ceramic matrix containing open, interconnected nanopores (1-100 nm), or simply called a ceramic "nano-foam" and (2) the actual penetration of metal into the nanopores. A research plan was developed to explore methodology of electrochemical and electroless depositions to achieve dense infiltration of metal into the pores of a nano-foam preform.

In regard to the preparation of a nanoporous ceramic matrix (i.e., the nano-foam), evaluation of the following concepts was performed:

- (1) anodized aluminum oxide (AAO), containing parallel channel pores (250 nm down to 10 nm), which can serve as a model system for study of infiltration and property measurements.
- (2) a molecular templating approach which might be good to produce layered, gel or powder type materials that contain micropores (<1 nm) and mesopores (2-50 nm).
- (3) a powder consolidation route to make nanoporous ceramics. (a novel concept that utilizes powders prepared by molecular templating via the biocontinuous phases of block co-polymers was also investigated in hopes of creating interconnected, open pores through the consolidated ceramic matrix)

Regarding low temperature electrochemical infiltration, a method was demonstrated at ORNL to deposit and accumulate a metallic phase into the nanopores of a ceramic substrate. This method improves upon the traditional method for fabrication of porous ceramic materials by ceramic powder pressing and sintering, which has the limitation of not being able to create uniform, interconnected, open pores of nanometer scale. To overcome this limitation, a novel fabrication method was developed that utilizes molecular self-assembly or microphase separation of block-copolymers, in combination with a controlled diffusion/evaporation scheme. Great success was obtained by this method based on preliminary results showing the achievement of a bulk-sized monolithic nanoporous solid matrix (see Figure 4) of ~25 mm diameter and 5 mm thickness. This matrix possesses the desired nanopore characteristics (i.e., nano-sized, interconnected, and open pores).

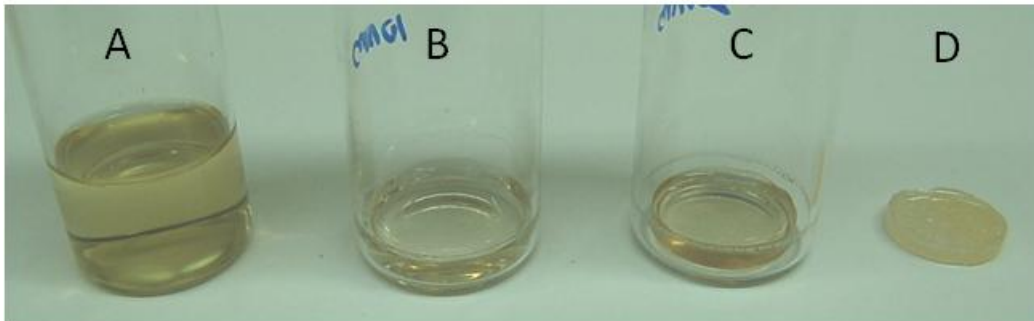


Figure 4. Example of controlled diffusion/evaporation during sol-gel and block-copolymer templated synthesis. (A) Initial liquid solution that contains mix of sol-gel inorganic precursors and block-copolymer template molecules. (B) A monolithic solid matrix is forming during liquid-to-solid transformation processing. (C) A completely formed dry solid matrix inside the molding reactor. (D) A free standing solid monolithic matrix that contains desirable interpenetrating, open nanopores.

Scanning Transmission Electron Microscope (STEM, Hitachi HD2000) images (Figure 5) for a specimen on a TEM grid, show the detailed pore nanostructure in lamellar, hexagonal, or mixed phases. The feature size of the mesophases is around 7.5 nm, which is determined by the nature of the template molecules (in this case, Pluronic P123 tri-block copolymers). Such pore nanostructures exist inside the bulk monolithic matrix.

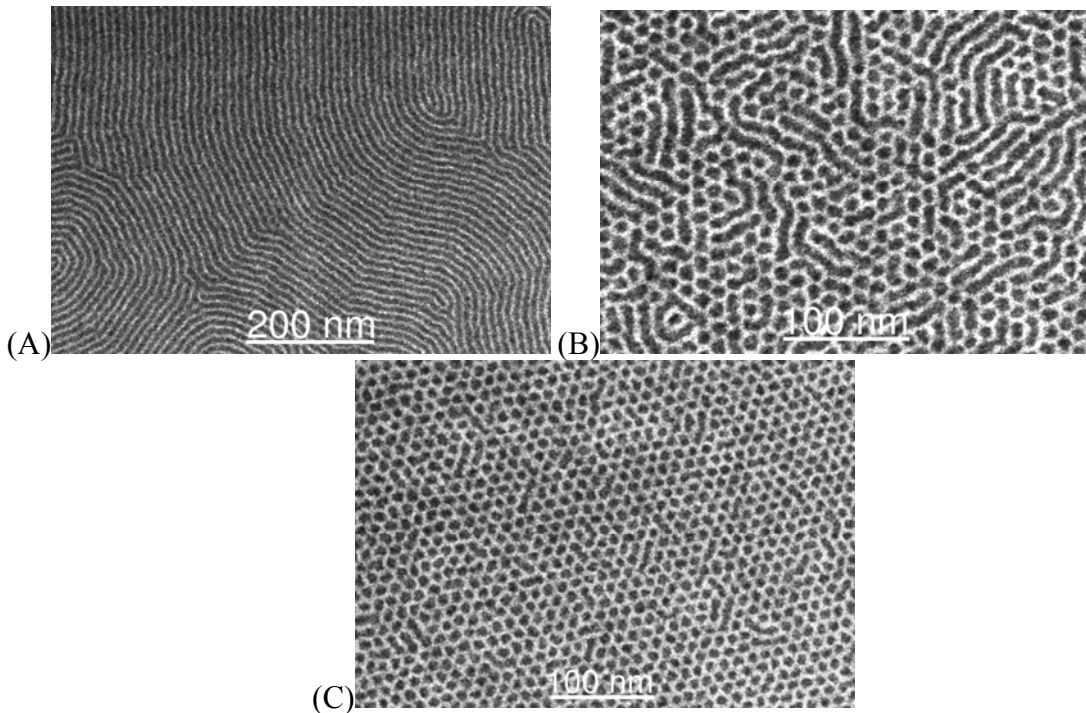


Figure 5. STEM images of nanopore nanostructures (7.5 nm , black areas) inside specimens on a TEM grid, prepared by block-copolymer templated sol-gel synthesis.

(a) lamellar microphase (b) mixed phase (c) hexagonal phase.

Note: darker lines or dots correspond to the nanopores, and the bright lines correspond to the inorganic (silica) matrix.

The greatest advantages of this method include:

- (1) Molecular-precision control of nanopore size, shape, and network morphology. Typically, the nanopore size can be flexibly tailored in the range of 2-50 nm by choosing different templating molecules.
- (2) Easy control of the shape of the monolithic solid matrix.
- (3) Good scalability of processing and matrix dimension.
- (4) Low cost of the approach.

Additional research is still needed to further understanding of the process parameters that affect the microphase control to ideally, achieve gyroid, cubic-phased interpenetrating nanopores. Engineering scale up studies are also needed to make practical sized nanoporous matrix materials.

Low-temperature routes to create co-continuous interpenetrating ceramic-metal (CICM) nano-composites were also evaluated. The focus was on the conceptual development of three promising routes.

- (1) Low temperature co-sintering of mixed ceramic and metallic nanopowders

In classical nanophase formation from nanopowders, sintering temperatures could be much lower than those used for conventional coarse-grained powders. A study of the literature showed that there is a lack of such co-sintering development, although there

are studies on processing of ceramic or metal nanocrystalline materials from nanopowders. From both a fundamental science and a nano-manufacturing point of view, the co-sintering formation phenomena of mixed ceramic-metal nanophases were looked into. The literature was also analyzed to identify the sintering temperature for ceramic nanopowders and for metallic nanopowders. This raised the observation that modeling could be used to identify the possible regime of conditions (based on nanopowder size, volume fraction of nanopowders, and sintering temperature) to warrant the co-continuous nanophase formation.

(2) Infiltration of metal into nanoporous cellular ceramics or ceramic nano-foams (such as anodized alumina or titania, sol-gel nano-foams or aerogels).

Challenges for this route were found to lie in the synthesis of the nano-foam of one phase (e.g. ceramic) and the infiltration of the other phase (e.g. metal). Only one preliminary work could be found that attempted a rudimentary ceramic nanopowder pressing/sintering technique to create a ceramic nano-porous matrix and electrochemical infiltration of a metal phase. To develop an advanced method for making “nano-foams”, the literature work on synthesis of ceramic foams and on aerogels was reviewed in hopes of identifying techniques to create and stabilize the cellular nanopore structures that enable thermal insulation properties. One of the greatest advantages of the nano-foam/aerogel route is the capability of making monolithic bulk size components. The key is to create a large enough metallic continuous nanophases inside a gel background. On the other hand, the anodized oxide in the form of thin films containing one-dimensional nanopore channels (see images below in Figure 6 of preliminary results on anodized alumina and titania samples made at ORNL) may serve as a model system to study mechanical or thermal properties.

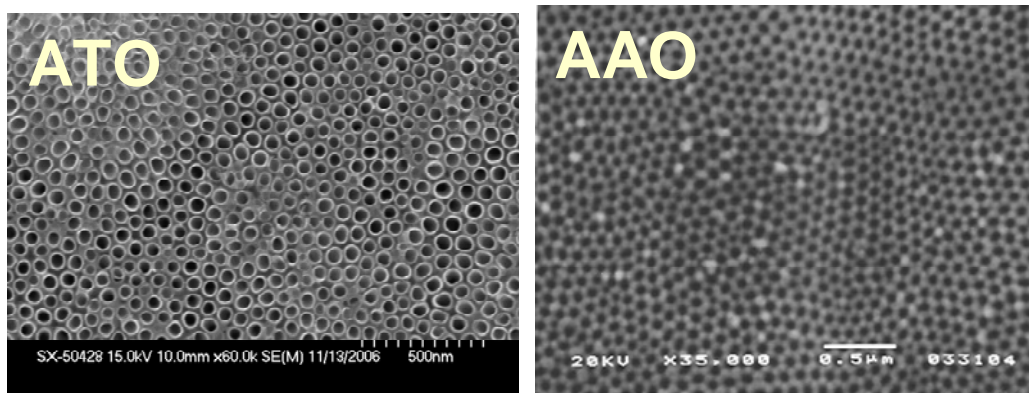


Figure 6. Nanopore channels in anodized aluminum oxide (AAO) and anodized titanium oxide (ATO).

(3) Co-formation of bi-continuous block copolymer microphases with ceramic and metal precursors

This is a novel concept for possible one-step chemical synthetic forming of CICM nanocomposites. The key is to distribute the ceramic and metal precursors separately into the separate hydrophobic or hydrophilic micro/meso phases that are “bi-continuous”. This route may create the most homogenous interpenetrating nanophases with well controlled nanophase dimensions and architectures. Note that when only one

micro/meso phase is incorporated with either ceramic or metal precursors, a homogeneous nanoporous ceramic or metal foam will be produced.

Bi-continuous phases which are thermodynamically stable phases per phase diagrams found for di- and tri-block copolymers (shown schematically in Figure 7) were also considered.²⁰⁻²⁴

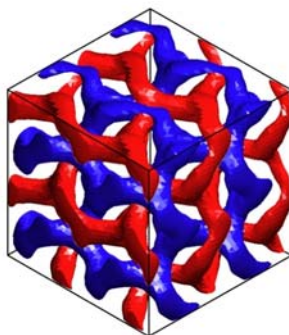


Figure 7. Schematic of bi-continuous phase structure

Efforts were conducted to:

- (1) Identify block-copolymer systems that favorably form bi-continuous phases (hydrophilic and hydrophobic or hydrophobic/hydrophobic), which include poly(isoprene-*b*-ethylene oxide) (PI-*b*-PEO)²⁵, poly(ethylene)-*b*-poly(ethylene oxide) (PE-*b*-PEO)²⁶, poly(styrene)-*b*-poly(ethylene oxide) (PS-*b*-PEO)²⁷, and PEO-*b*-PPO-*b*-PEO²⁸.
- (2) Identify suitable (hydrophilic/hydrophobic) ceramic precursors and (hydrophilic/hydrophobic) metal precursors, which could be distributed (via partition or covalent linking) in the corresponding bi-continuous phases. A few examples of currently studied precursors include Ormocer precursors (3-glycidyloxypropyl)-trimethoxysilane and aluminum sec-butoxide to produce aluminosilicate with a mesostructured continuous pore²⁵, tetraethyl orthosilicate (TEOS) or tetramethyl orthosilicate (TMOS) to produce mesostructured silica such as MCM-48²⁸⁻³¹, alkoxide Ti(OC₃H₇)₄ to produce titania²⁸, Homo-PS to produce mesostructured polystyrene³², palladium nanoparticles to create a high specific surface area material composed of palladium nanoparticles distributed in a poly(2-vinylpyridine) double gyroid network texture³³, and metal coated connected nanochannels³².
- (3) Justify the forming possibility of the dense bi-continuous phases in ceramic/ceramic or ceramic/metal, or metal/metal nanocomposites. Currently, there are no studies that demonstrated dense nanocomposite phases. In principle, if sufficient concentration of inorganic (ceramic or metal) precursors are distributed into the corresponding bi-continuous phases, they could be further densified, while maintain the bi-continuous skeleton architecture.

5.2 Investigation of High Temperature Processes for IPC Production

The following work was performed to determine the technical and economic feasibility of producing nano-scale IPC components of a useable size by modification of the alternative high temperature method. For the high temperature process, initial efforts were centered

on reducing the length scale of produced TCON materials through metallic additions to form intermetallic phases. Previous work indicated that there is promise in the use of metallic additions to successfully form IMC phases with features on the nano-scale¹⁸. Methods of incorporating such additions into materials formed by the TCON process were therefore sought. It was determined that additions could successfully be made through the use of metal alloys obtained through a commercial supplier (Milward Alloys, Inc., Lockport, NY) as master alloys. Alloys of aluminum-silicon (Al-Si), aluminum-iron (Al-Fe), aluminum-titanium (Al-Ti), and aluminum-magnesium (Al-Mg) were therefore obtained.

Work was also focused on the choice of preforms. Alternative preforms to the fused silica normally used in the TCON process were sought with nano-scale grain size or features. Yet, existing preform materials with nano-scale grain size or features were not found to be readily commercially available. Therefore, sources of experimental materials were sought. One such source was found to be Pacific Northwest National Laboratory (PNNL) where Dr. R. Shane Addleman of the Functional Multiscale Materials Group has performed work regarding the production of three dimensional cellulose template mesoporous silica macrostructures and nanoporous ceramic substrates as shown in Figure 8³⁴. Such materials can be produced out of silica, titania or zirconia and are thought to possibly be suitable as substrates for the TCON process or possibly for use in the low temperature process in future work.

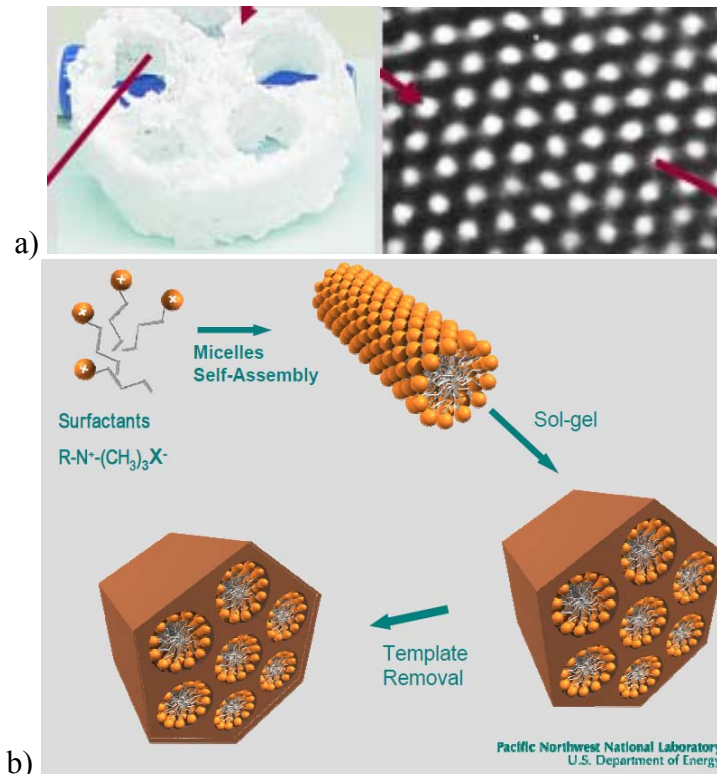


Figure 8. Examples of PNNL mesoporous and nanoporous substrate production showing a mesoporous silica macrostructure (a) and a route to a nanoporous ceramic substrate (b)³⁴.

In other efforts to explore alternative preform materials, a meeting was held between fused silica supplier Momentive Performance Materials (Strongsville, OH) and ORNL. Through these discussions and those by Fireline with their normal preform supplier (Technical Glass Products, Painesville, OH) several possible fused quartz and Vycor™ glass materials were identified. Additionally, other preforms composed of either clay (produced in-house by Fireline) or a proprietary material being developed by Youngstown State University (YSU) were also identified.

The detailed mechanisms of the transformation process (mass transfer rate, diffusion, and reaction kinetics) were also investigated. Additionally, alternative processing methods such as plasma processing, increased reaction rates, and alternative mechanisms were considered. The processing variable of transformation time was identified as the most likely to affect the resulting microstructure of the final transformed material, therefore variation of this value was selected to see if it had an effect on the produced micro-/nano-structure.

A matrix of the initial planned sample runs is shown in Table 8. A minimum of two samples were transformed for each test run condition.

Table 8. Matrix for TCON Sample Preparation

Run #	Preform Material	Metal Addition	Transformation Time
1	Clear fused quartz	Al-25%Si	6 hours
2	Clear fused quartz	Al-25%Si	24 hours
3	Clear fused quartz	Al	6 hours
4	Clear fused quartz	Al-7.5%Fe	4.63 hours
5	Clear fused quartz	Al-3%Ti	4.83 hours
6	Clear fused quartz	Al-2.5%Mg	23.5 hours
7	Vycor glass	Al	2 hours and 4 hours
8	Clay body	Al	8 hours
9	Vycor glass	Al-3%Ti	8 hours
10	YSU proprietary	Al	6 hours

Sample Runs #1-9 were completed by Fireline. Samples planned in Run #10 using the YSU proprietary preform (later identified as a zeolite material) did not transform. Pictures of prepared samples are shown in Figure 9.

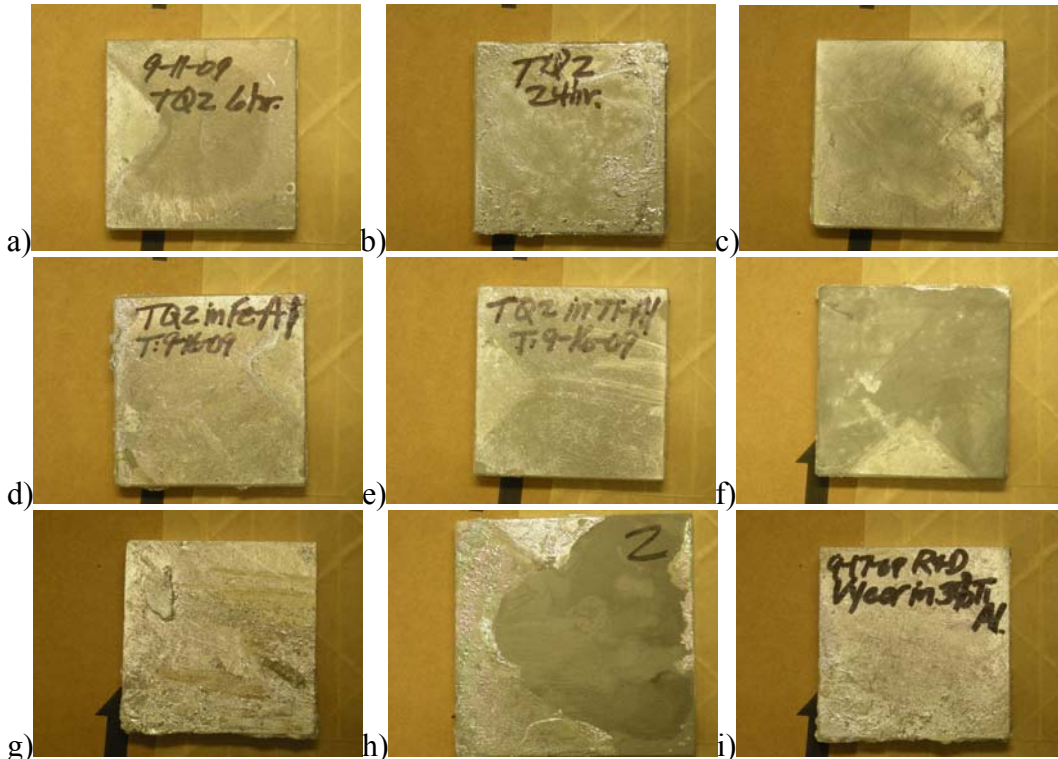


Figure 9. Pictures of prepared experimental TCON samples from Run #1 (a), #2 (b), #3 (c), #4 (d), #5 (e), #6 (f), #7 (g), #8 (h), and #9 (i).

Upon receipt at ORNL, samples were sectioned to produce three types of specimens. Standard bend bars (50.8 mm x 6.35 mm x 4.01 mm) were cut for basic mechanical testing. Square sections (12.7 mm x 12.7 mm x 6.35 mm) and rectangular sections (12.7mm x 6.35mm x 6.35mm) were also removed to analyze the microstructures parallel and perpendicular to the plate surface, respectively. Samples were analyzed by optical microscopy, SEM, and TEM to determine features and length-scale of the resulting materials.

Four-point bend testing (per ASTM C1161³⁵) was performed to analyze change in mechanical properties of samples produced using metallic additions, alternative performs, and alternative processing conditions (as defined in Table 8); compared to standard TCON materials produced under normal processing conditions. Flexure values were calculated using Equation 2.

$$S = \frac{3PL}{4bd^2} \quad (2)$$

where: S = flexure strength
P = breakload
L = outer (support) span
b = specimen width
d = specimen thickness

Values for flexure strength of standard grade TCON have previously been determined at ORNL and reported by Fireline as ~170 MPa (25 ksi)³⁶. Measured values and standard deviations (for three measured samples) for materials produced through the nine experimental runs are shown in Table 9 and are plotted in Figure 10.

Table 9. TCON Flexure Strength Values

Sample Run	Condition	Flexure Strength MPa (ksi)	Standard Deviation MPa (ksi)
1	FQ/Al-25%Si/6 hr.	192.57 (27.93)	23.37 (3.39)
2	FQ/Al-25%Si/24 hr.	205.19 (29.76)	8.55 (1.24)
3	FQ/Al/6hr.	170.78 (24.77)	8.69 (1.26)
4	FQ/Al-7.5%Fe/4.63 hr.	239.52 (34.74)	35.71 (5.18)
5	FQ/Al-3%Ti/4.83 hr.	210.84 (30.58)	13.31 (1.93)
6	FQ/Al-2.5%Mg/23.5 hr.	234.00 (33.94)	21.37 (3.10)
7	V/Al/2 hr. V/Al/4 hr.	190.09 (27.57) 116.87 (16.95)	3.38 (0.49) 1.03 (0.15)
8	C/Al/8 hr.	95.91 (13.91)	28.54 (4.14)
9	V/Al-3%Ti/8 hr.	164.03(23.79)	62.54 (9.07)

(Condition code = preform material/metal addition/transformation time (in hours))
(FQ = fused quartz, V = Vycor™ glass, C = clay)

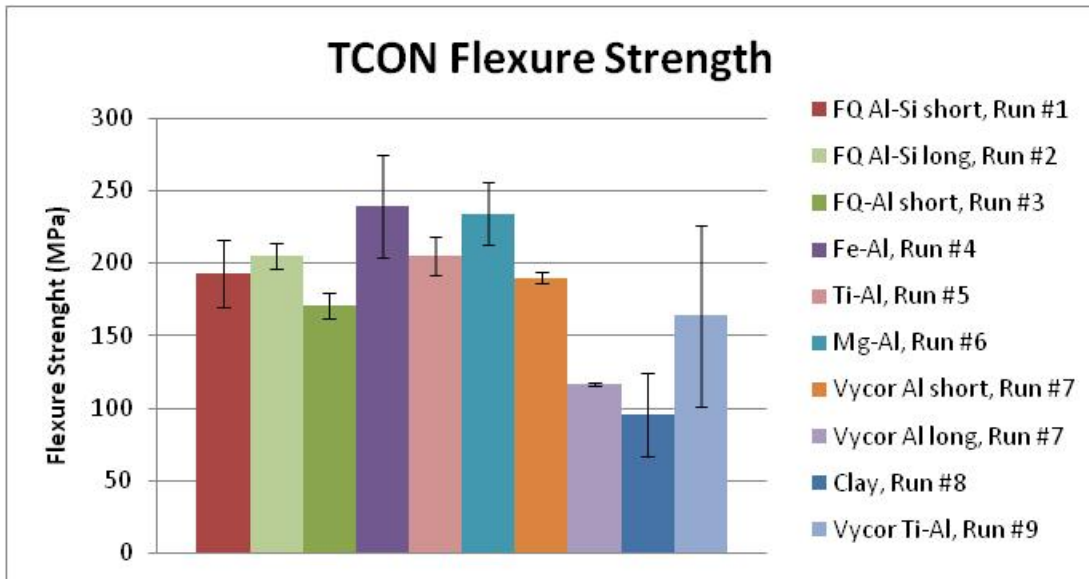


Figure 10. TCON flexure strength vs. sample run and processing conditions. (Error bars show standard deviation of three tested samples)

Runs #1 and #2 represent the standard TCON formulation processed with the addition of Al-25%Si alloy in place of pure Al and for short (6 hours) and long (24 hours) transformation times, respectively. Samples for these two conditions were found to have similar flexure strength values to one another (193 and 205 MPa with standard deviations of ~23 and 8.5 MPa). The similar values for these two conditions indicate that transformation time did not appear to affect the microstructure in a manner that affected

the strength of the material. These two samples both exhibited slightly higher strengths than Run #3, a standard TCON formulation that was processed with a short transformation time (6 hours) using pure aluminum. The measured flexure strength for Run #3 (~170 MPa, 9MPa standard deviation) was within the standard deviation of Run #1, indicating that transformation time did not appear to affect the microstructure in a manner that affected the strength of the material, yet the addition of silicon to the transformation bath may slightly increase the strength of the resulting IPC.

Run #4 uses an Al-7.5% Fe alloy in place of pure Al and short transformation time (4.63 hours). As expected the addition of iron increases the flexure strength of the resulting IPC considerably to a level of nearly 240 MPa (~35 MPa standard deviation). Similarly, the use of Al-2.5%Mg alloy in place of pure Al (Run #6) produces an IPC with a flexure strength of nearly 235 MPa (~21 MPa standard deviation), although longer transformation times (23.5 hours) were required to fully transform the samples. Run #5 which uses Al-3%Ti in place of pure Al and a short transformation time (4.83 hours) produced weaker samples with a flexure strength on the order of 210 MPa (~13 MPa standard deviation), but still slightly stronger than TCON in the Al-Si transformation run. It can also be noted that materials incorporating titanium are similar in strength to those incorporating silicon (Run #1 and #2).

Run #7 uses a Vycor™ glass preform in place of fused quartz and pure Al metal similar to that used for transformation of standard TCON material. Since it had been shown previously that transformation time did not appear to affect the resulting IPC, only short transformation times were used. Initial samples were produced using a 4 hour transformation time, but the quality of the transformation was questionable (transformation time deemed to be too long). A second run was performed using a 2 hour transformation time. Flexure strength of the 4 hour transformation samples was found to be 117 MPa with a 1 MPa standard deviation. Flexure strength of the 2 hour transformation samples was found to be 190 MPa with a 3 MPa standard deviation. This confirmed that poor transformation occurred for the 4 hour samples. Again, it can be noted that the strength of the 2 hour samples is similar to that of materials from Runs #1 and #2 (fused quartz preforms processed with Al-Si alloy) and from Run #5 (fused quartz preforms processed with Al-Ti alloy) and is slightly higher than that of standard TCON material indicating that the use of Vycor™ glass preforms instead of fused quartz may lead to slightly increased strength.

Run #9 was performed using Vycor™ glass preforms, Al-3%Ti alloy, and a moderate length (8 hour) transformation time. Difficulty was experienced, even with this longer transformation time, in successfully transforming these samples. The flexure strength of these samples was found to be low and to vary greatly between test pieces at 164 MPa with a standard deviation of over 60 MPa. Further investigation into transformation times would be necessary to fully develop this material.

Run #8 uses a clay preform material in place of fused quartz and pure Al metal similar to that used for transformation of standard TCON material. Initial interest in the use of clay preforms was due to the nano-structure inherently present in kaolinite ($\text{Al}_2\text{Si}_2\text{O}_5(\text{OH})_4$). A

4 hour transformation time and low sintering temperatures were used for the production of these samples in an effort to retain the original clay structure. Although the samples fully transformed, there was a large degree of porosity in the final IPC structure (over 20% as compared to 0-10% found in typical TCON materials) as evident in the sample cross section shown in Figure 11.

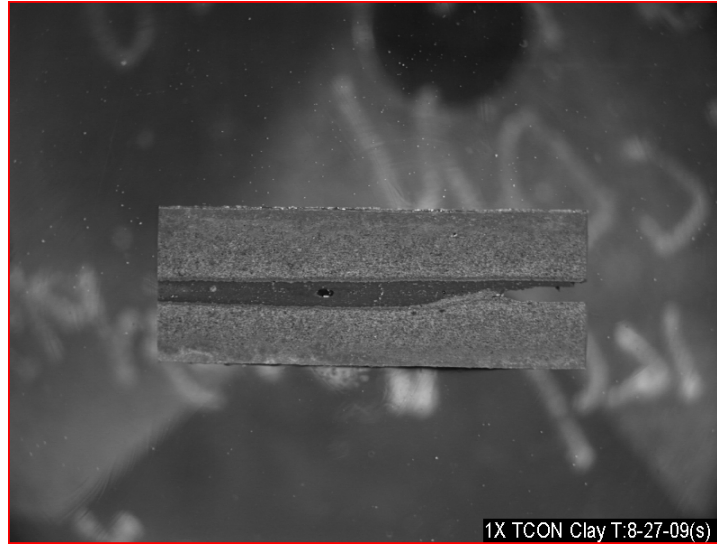


Figure 11. Optical microscopy of clay preform (Run #8) sample cross section exhibiting large porosity of transformed sample.

The relative open structure of these materials is expected to have led to a decrease in the mechanical properties of this material resulting in measured flexure strength of only 95 MPa and relatively high variability between test pieces (standard deviation of nearly 30 MPa).

Microscopy samples were first analyzed by SEM to identify selected areas of interest. Once areas were identified, a Focused Ion Beam (FIB) was used to mill samples for TEM analysis. TEM analysis was then used in an effort to evaluate the length scale of the various formed materials along with composition of the phases that were present.

Figure 12 shows TEM images of material produced using the Al-Si alloy in place of pure Al (Run #2). This sample was found to be composed of an alumina phase with isolated Al metal particles (dark regions in the alumina phase field) and an Al metal phase. The grain size of the two major phases was found to be on the micron-scale, as opposed to the nano-scale. Si was not found during the TEM analysis. This microstructure is similar in structure and scale to that of the standard TCON material as shown in Figure 3(a) and is consistent with the only slight increase in strength exhibited by this material compared to standard TCON. TEM analysis of material from Run #1 (material produced using the Al-Si alloy in place of pure Al and a shorter transformation time) produced similar results, therefore they are not shown.

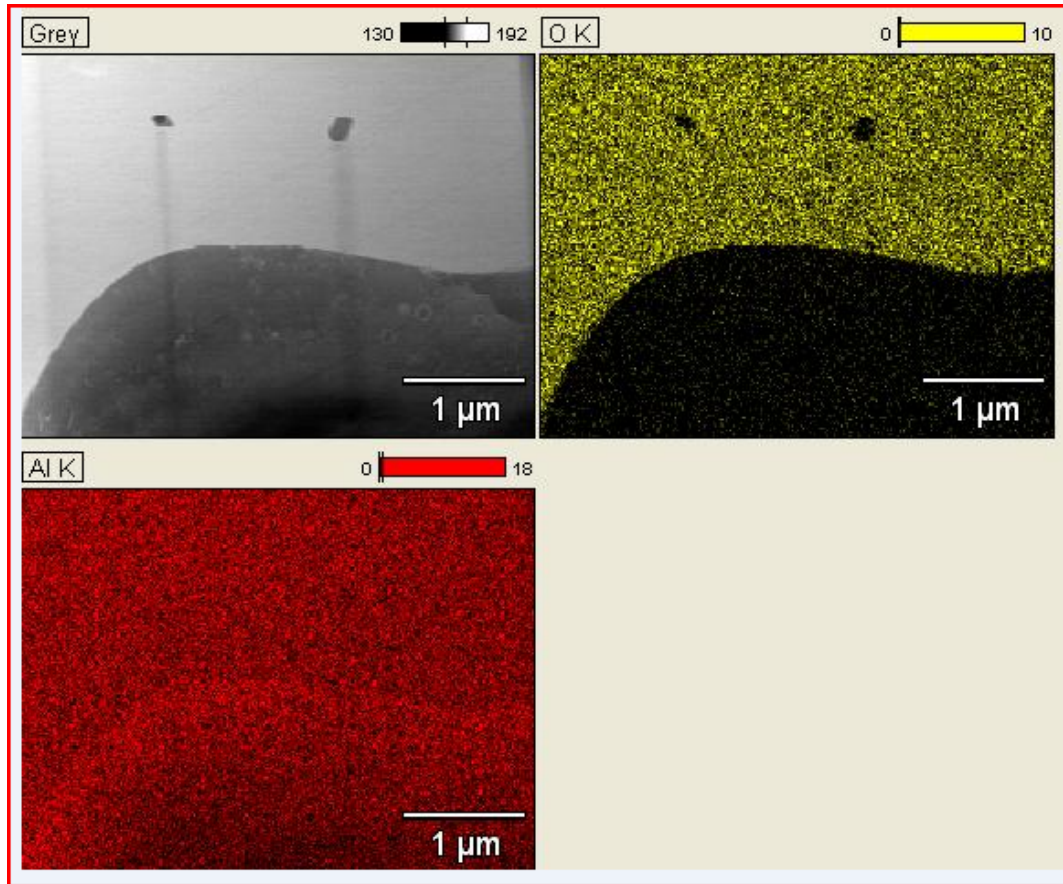


Figure 12. TEM images of Run #2 sample (fused quartz/Al-25%Si alloy/24 hour transformation time).

An SEM image of the material produced using the Al-Fe alloy in place of pure Al (Run #4) is shown in Figure 13 (a). The alumina grain size (raised features) was still found to be on the micron level, while the secondary Al metal phase which is expected to contain the Al-Fe intermetallic phase (recessed features) appears to possibly be sub-micron. This was confirmed through TEM analysis as shown in Figure 13 (b) where the alumina and Al metal phases were found to be on the micron scale (as identified above), but the Al-Fe intermetallic compound phase (IMC) was found to possess nano-scaled features. It is expected that this nano-scaled phase contributes to the increase in strength exhibited by this material.

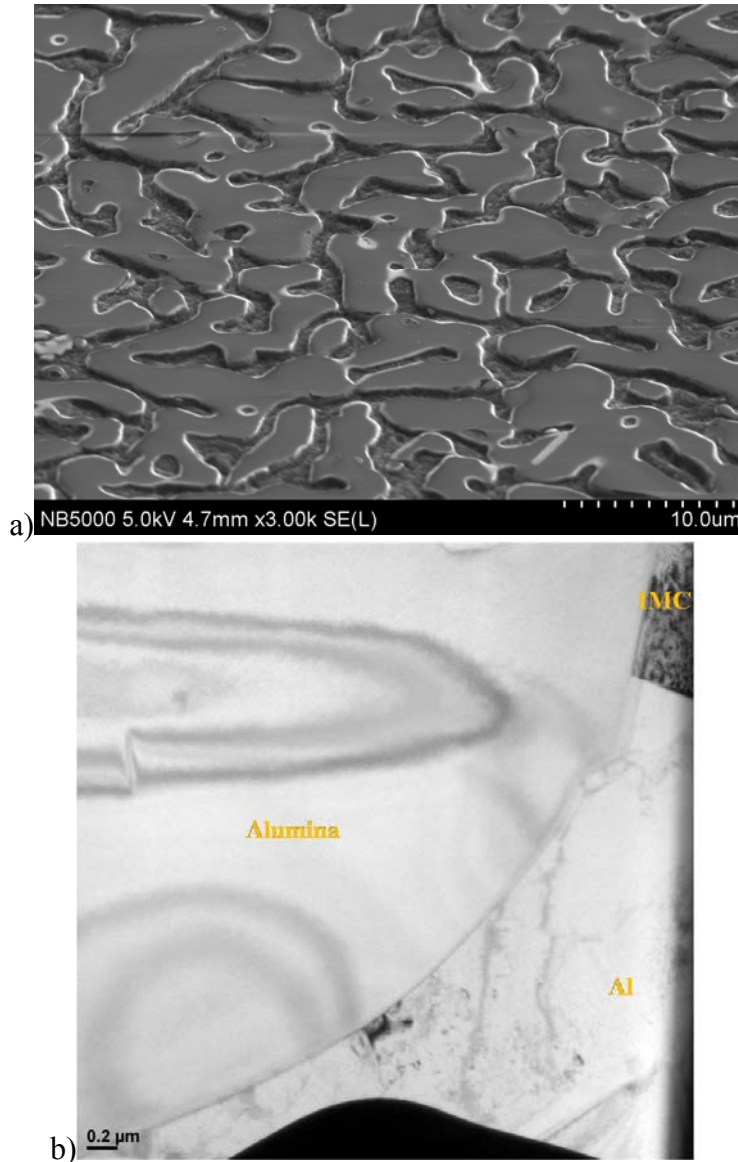


Figure 13. SEM (a) and TEM (b) images of Run #4 sample (fused quartz/Al-7.5%Fe alloy/4.63 hour transformation time).

Figure 14 shows a TEM image of material produced using the Al-Ti alloy in place of pure Al (Run #5). Analysis of this material did not reveal the expected Al-Ti intermetallic phase that was hoped to be formed leading to increased strength being exhibited by this material. The only observed phases were alumina particles and Al metal matrix (note the Al metal phase was found to contain ≤ 1 at% Ti) consistent with the microstructure of standard TCON material. This may explain why only a slight increase in strength was exhibited by this material compared to standard TCON material.

TEM images of the material produced using Al-Mg alloy in place of pure Al (Run #6) are shown in Figure 15. This material displayed nano-scaled spinel ($\text{MgO-Al}_2\text{O}_3$) particles in an Al metal matrix. It is expected that the solid solution spinel phase is what contributes to the increased strength exhibited by this material compared to standard TCON material.

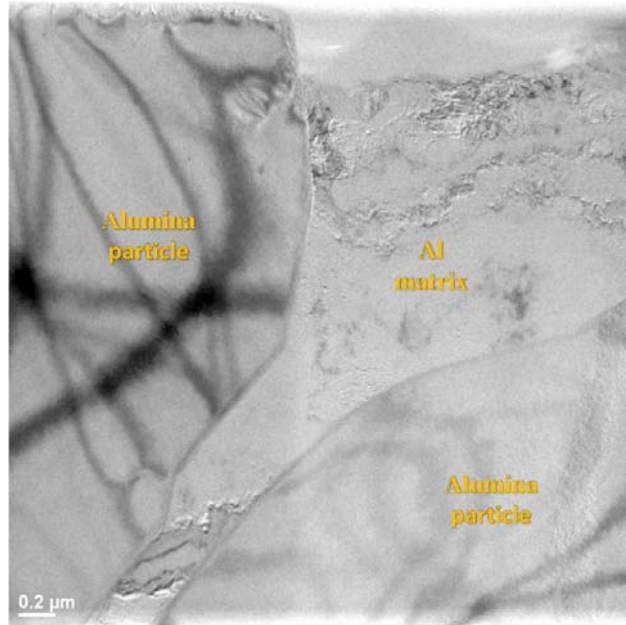


Figure 14. TEM image of Run #5 sample (fused quartz/Al-3% Ti alloy/4.83 hour transformation time).

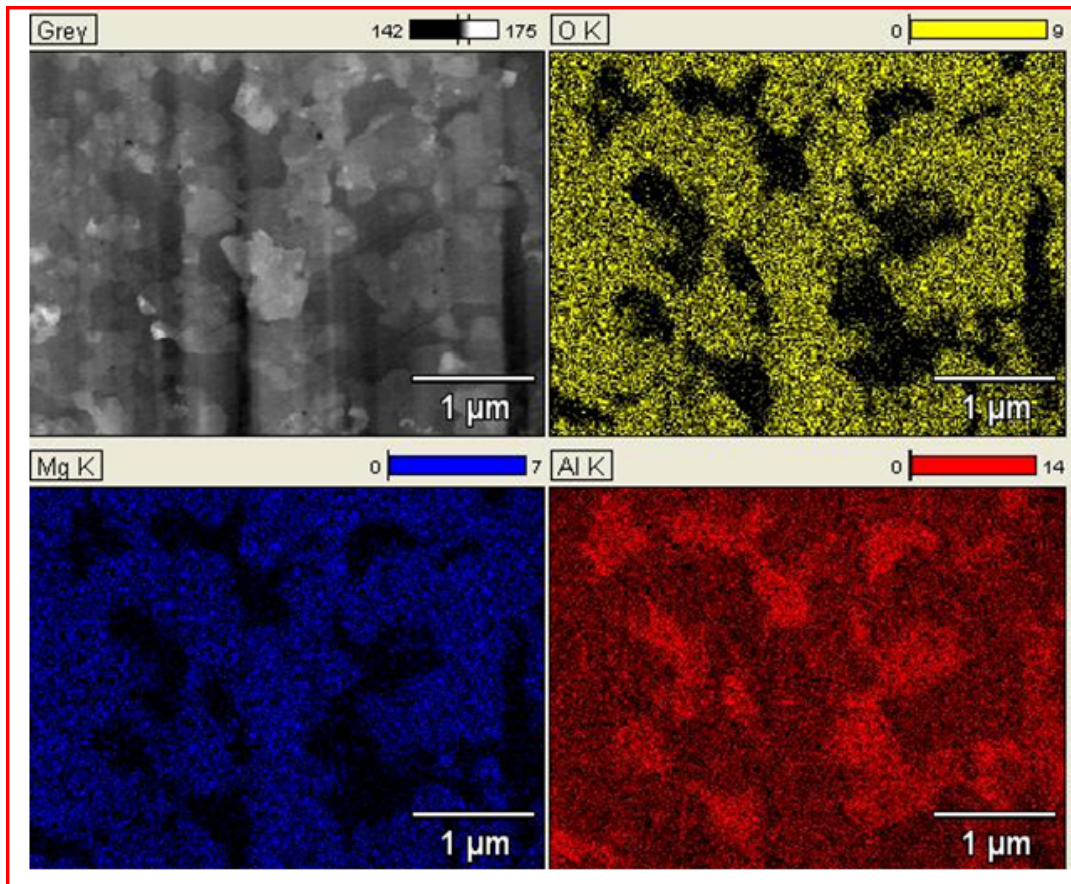


Figure 15. TEM images of Run #6 sample (fused quartz/Al-2.5%Mg alloy/23.5 hour transformation time).

A TEM image of the material produced using pure Al and a Vycor™ glass preform in place of fused quartz (Run #7) is shown in Figure 16. Two phases were identified through the TEM analysis. The first was composed of alumina particles (0.5 to > 1.0 micron). These particles were in an aluminum matrix which exhibited low-angle grain boundaries, but was not necessarily nano-scaled. Yet, the presence of these smaller features differentiates it from the microstructure exhibited by standard TCON material (as seen in Figure 3(a)) and may lead to the slightly increased strength exhibited by this material compared to that of standard TCON.

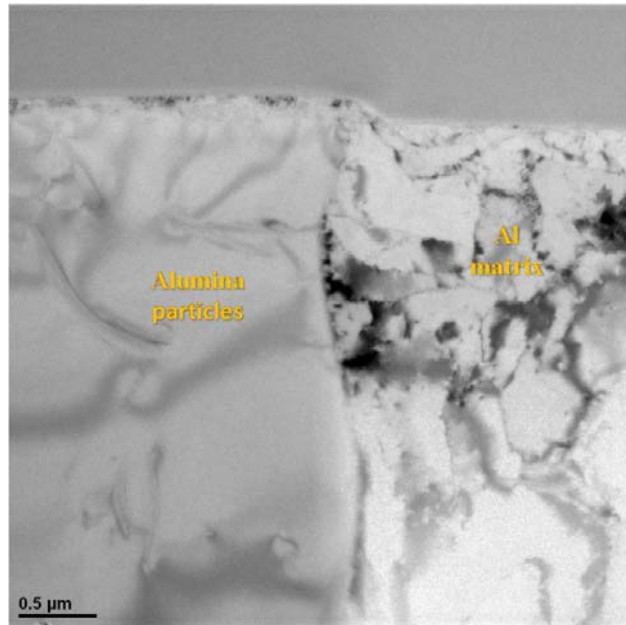


Figure 16. TEM image of Run #7 sample (Vycor™ glass/pure Al /2 hour transformation time).

Figure 17 shows TEM images of material produced using pure Al and a clay preform (Run #8). Analysis only identified alumina particles in a Si metal matrix. Surprisingly no residual silica from the kaolinite ($\text{Al}_2\text{Si}_2\text{O}_5(\text{OH})_4$) clay preform was found during the TEM analysis. The alumina particles were found to still be nano-scaled, but any increases in strength due to this scaling were lost due to the large degree of porosity in the final IPC structure noted above. If this porosity could be eliminated, increased strengths may still be possible for this material.

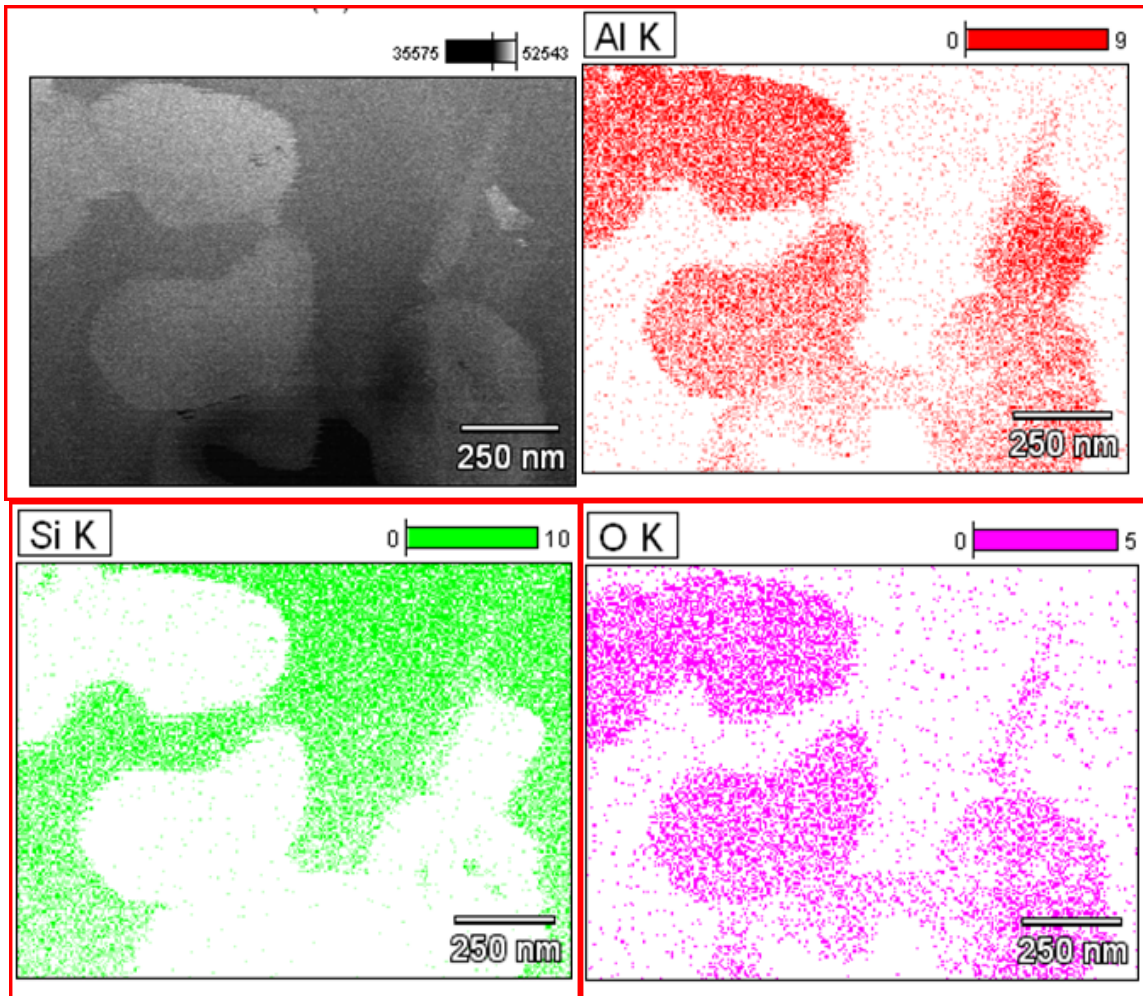


Figure 17. TEM images of Run #8 sample (clay/pure Al /8 hour transformation time).

5.3 Project Milestones

The following milestones were set for this project. Times shown were in reference to the start of the project. All milestones were met as indicated in the Summary section below.

- (1) 6 months – determination of feasibility of producing nano-scale IPC's by the low temperature process with improved metal infiltration and wetting and by the high temperature process with reduced length scale due to metal additions
- (2) 9 months – determination of feasibility of scaling low temperature process and modifying preform or processing conditions in high temperature process
- (3) 12 months – determine properties of produced components

5.4 Lux Research Activities

Throughout the project, discussions were held with Lux Research (New York, NY) regarding their collaboration (through separate DOE funding) on finding industrial partners and defining applications and potential markets or materials developed under this project. Several teleconferences were held between ORNL and Lux to discuss a

report they were preparing regarding routes to market, near-term applications, potential commercial challenges, and possible partnerships related to this project. This report was based on discussions between ORNL and Lux, discussions between Lux and Fireline, and independent research performed by Lux. Comments and revisions were supplied to Lux throughout the project for inclusion in the report which was scheduled to be issued sometime during 2010.

6. Summary

- It was determined through literature review and preliminary experimental results at ORNL that it appears improved nano-scale IPC materials can be produced through identified improved low temperature metal infiltration and wetting techniques (Milestone #1 of the project). Additionally size scaling of materials produced by these improved low temperature methods is believed to be possible based on preliminary results achieved at ORNL (Milestone #2 of the project).
- One identified route for production of IPC materials by low temperature methods was the infiltration of metal (such as Cu, Al, or an alloy) into a nanoporous ceramic matrix (such as alumina, silica, or titania). It was determined that the greatest challenges to such a method included: (1) the creation of a nanoporous ceramic matrix containing open, interconnected nanopores (1-100 nm), or simply called ceramic “nano-foam” and (2) the actual penetration of metal into the nanopores.

Regarding the preparation of a nanoporous ceramic matrix (i.e. nano-foam), anodized aluminum oxide containing parallel channel pores (250 nm down to 10 nm) was investigated which can serve as a model system for study of infiltration and property measurements. Using this material, a molecular templating approach might be possible to produce layered, gel or powder type materials that contain micropores (<1 nm) and mesopores (2-50 nm) or a powder consolidation route may be possible to make nanoporous ceramics.

Regarding low temperature electrochemical infiltration, a method was demonstrated at ORNL to deposit and accumulate a metallic phase into the nanopores of a ceramic substrate. This method improves upon the traditional method for fabrication of porous ceramic materials by ceramic powder pressing and sintering, which has the limitation of not being able to create uniform, interconnected, open pores of nanometer scale. Low-temperature routes to create co-continuous interpenetrating ceramic-metal (CICM) nano-composites were also evaluated. The focus was on the conceptual development of three promising routes: 1) low temperature co-sintering of mixed ceramic and metallic nanopowders, 2) infiltration of metal into nanoporous cellular ceramics or ceramic nano-foams, and 3) co-formation of bi-continuous block copolymer microphases with ceramic and metal precursors.

- It was also determined through literature review, discussions with Fireline, and preliminary results that TCON materials may be possible with nano-scaled features through the use of the alternative high temperature process coupled with the use of metallic additions to produce intermetallic compound (IMC) or solid-solution (spinel for example) phases (Milestone #1 of the project). Although, the processing conditions (duration of transformation time) altered in this work did not lead to

reduction of the length scale of TCON materials, preform materials were identified which may lead to such reductions of the length scale from the micro-scale to the nano-scale (Milestone #2 of project).

- Samples were prepared, some exhibiting nano-scale and increased strengths, using the alternative high temperature process incorporating various metallic additions, alternative preform materials, and varying processing times. Samples representing the standard TCON formulation processed with the addition of Al-25%Si alloy in place of pure Al for short and long transformation times (Runs #1 and #2) were found to have similar flexure strength values to one another and showed only slightly higher strength than standard TCON. Microstructural evaluation confirmed these findings. Therefore it was concluded that the addition of silicon may increase the strength of the resulting IPC, but only slightly and that transformation time did not appear to affect the microstructure in a manner that affected the strength of the material. These two samples both exhibited slightly higher strengths than a standard TCON formulation that was processed with a short transformation time using pure aluminum (Run #3). The measured flexure strength of this material was within the standard deviation of Run #1, indicating that transformation time did not appear to affect the microstructure in a manner that affected the strength of the material, yet the addition of silicon to the transformation bath may slightly increase the strength of the resulting IPC.

Samples with Al-7.5% Fe alloy in place of pure Al and short transformation time (Run #4) showed a considerable increase in flexure strength due to the addition of iron and the formation of a nano-featured intermetallic compound (IMC) phase. Similarly, the use of Al-2.5%Mg alloy in place of pure Al (Run #6) produced an IPC with nanostructure and increased flexure strength, although longer transformation times were required to fully transform this material and form the needed solid solution phase. Material which was produced using Al-3%Ti in place of pure Al and a short transformation time (Run #5) was found to be weaker in flexure strength, but still slightly stronger than standard TCON. TEM analysis of this material did not reveal the expected Al-Ti intermetallic phase that was hoped to be formed leading to increased strength being exhibited by this material. This was consistent with the only slight increase in strength exhibited by this material compared to standard TCON material.

Material produced using a Vycor™ glass preform in place of fused quartz and pure Al metal similar to that used for transformation of standard TCON material (Run #7) was found to show a flexure strength similar to that of materials produced using fused quartz preforms processed with Al-Si alloy and materials produced using fused quartz preforms processed with Al-Ti alloy. The flexure strength of this material was only slightly higher than that of standard TCON material indicating that the use of Vycor™ glass preforms instead of fused quartz may lead to only slightly increased strengths. These results were confirmed by TEM analysis which showed the presence of smaller features differentiating it from the microstructure exhibited by standard TCON material which may lead to the slightly increased strength exhibited by this material compared to that of standard TCON. Materials produced using Vycor glass

preforms, Al-3%Ti alloy, and a moderate length transformation time (Run #9) showed difficulty in successfully transforming. The flexure strength of these samples was found to be low and to vary greatly between test pieces. Further investigation into transformation times would be necessary to fully develop this material.

Material produced using a clay preform material in place of fused quartz and pure Al metal similar to that used for transformation of standard TCON material (Run #8) also showed a difficulty in fully transforming. This resulted in a large degree of porosity in the final IPC structure (over 20% as compared to 0-10% found in typical TCON materials). The relative open structure of these materials is expected to have led to a decrease in the mechanical properties of this material resulting in a low measured flexure strength and relatively high variability between test pieces. If this porosity could be eliminated, increased strengths may still be possible for this material.

7. Suggested Follow-On Activities

This project only involved concept definition work to determine the feasibility of producing useable nanocomposite functional materials for implementation in industrial and vehicle applications. From the results of the project, it appears that such materials are possible using both concepts from the low- and high-temperature approaches investigated. It is thought that through a larger follow on project encompassing further concept development, technology development, and field verification activities, these materials could be brought to a point suitable for dissemination and commercialization by the project's industrial partner Fireline and other commercial partners. Applicable activities that could help lead to such a commercial realization of these materials are briefly discussed below.

Although no suitable nanoporous substrate materials were found to be commercially available, two possible future sources were identified. The first was commercially available material produced by NanoPore, Inc. (Albuquerque, NM)³⁷. NanoPore produces thermal insulation materials composed of silica, titania, and/or carbon in a three-dimensional, highly branched network of primary particles (2-20 nm) which aggregate into larger (nm to mm) sized particles leading to pore sizes ranging from 10-100 nm. Two grades of material are listed on the company website, a low temperature version (HP-150) for $T < 300^{\circ}\text{C}$, and a high temperature version (HP-170) for $T < 800^{\circ}\text{C}$. Custom grades of material are listed as also possibly being available for special project needs. Upon contacting NanoPore in April of 2009, it was learned that the company is currently only producing a low temperature version of this material which is composed of opacified carbon and is only rated for $T < 500^{\circ}\text{C}$. Yet, higher temperature versions may be pursued again and available at a later date. Future collaboration with NanoPore could lead to advances in this area and suitable substrate materials for nano-scale IPC materials produced by both the low- and high-temperature approaches.

The second possible source of nano-porous substrate material is the experimental materials identified previously in this document being produced at Pacific Northwest National Laboratory (PNNL) by Dr. R. Shane Addleman. These are three dimensional

cellulose template mesoporous silica macrostructures and nanoporous ceramic substrates which can be produced out of silica, titania or zirconia. Correspondence with Dr. Addleman indicated that he is currently making nano/mesoporous materials of various compositions, sizes and shapes. Powders, thin films, and monoliths have been produced and through adjustment of surface chemistry these materials can be tailored for specific applications. Again, future collaboration with PNNL could lead to advances in this area and suitable substrate materials for nano-scale IPC materials produced by both the low- and high-temperature approaches. Further work could also be pursued at ORNL to produce such materials.

The follow on research and development efforts for low temperature routes include infiltration of nanoporous ceramic foam and in-situ one-step formation of bi-continuous metal-ceramic phases. Challenging issues are the fundamental understanding and control of metal wetting into nanopores, the co-sintering phenomena of mixed metal and ceramic nanoparticles, and molecular template sol-gel formation of ceramic nanofoam and bi-continuous metal-ceramic phases. Synthesis and processing conditions need to be further developed for bulky dimension of solid nano-scale IPC's.

The concept of IPC materials produced by microphase separation was one successful low-temperature technique that was identified for the production of bulk-sized nanocomposite materials. Similarly, co-sintering of ceramic/metal nanoparticles was another low-temperature technique identified for the production of bulk-sized nanocomposite materials. Yet, additional work is needed to further develop these concepts.

Although nano-scaled IPC materials of a useable size were demonstrated in this project through the use of the high temperature processing method incorporating metallic additions and alternative preforms, further development and characterization of these materials is needed to understand how the property enhancements are facilitated by the reduction in structural scale. In addition, pursuit of materials produced using other inter-metallic phases, alternative preforms, and alternative processing techniques could lead to materials of different compositions which demonstrate increased corrosion resistance, improved mechanical properties, and faster/cheaper manufacturing (manufacturing efficiency).

Once materials are produced, work is needed to demonstrate implementation and validation of the nano-scaled IPC materials in industrial and automotive applications. This would involve teaming with additional industrial partners such as metal producers, glass producers, and vehicle brake manufacturers/users to provide testing in actual service applications. Such things as increased component lifetime, increased production through-put, process energy efficiency, reduced component weight, and energy/fuel consumption could be measured as bench marks of component performance.

Finally, following material validation, efforts must be made to disseminate information regarding these new materials to the various industries that could benefit from their use and full commercialization efforts must be undertaken.

8. Acknowledgements

The authors would like to acknowledge the U.S. Department of Energy (DOE) Office of Energy Efficiency and Renewable Energy (EERE) Industrial Technologies Program (ITP) who funded this work under DOE Award Number NT08840 (DOE Program Manager – Joseph Renk). TCON materials were produced by Fireline TCON, Inc. (Youngstown, OH). TCON sample preparation was performed by Randy Parton and Hu Longmire. TEM sample preparation and SEM analysis was performed by Dorothy Coffee. TEM analysis was performed by Karren More. The authors would also like to thank Fei Ren and Peter Blau for reviewing the manuscript.

9. References

1. J.G. Hemrick and K.M. Peters, "Advanced Ceramic Composites for Molten Aluminum Contact Applications", UNITECR' 09 Proceedings, Salvador, Brazil, October (2009).
2. K.M. Peters, R.M. Cravens, and J.G Hemrick, "Advanced Ceramic Composites for Improved Thermal Management in Molten Aluminum Applications", Energy Technology Perspectives: Conservation, Carbon Dioxide Reduction and Production from Alternative Sources, TMS, February (2009).
3. J.G. Hemrick, H.W. Hayden, P. Angelini, R.E. Moore, and W.L. Headrick, "Refractories for Industrial Processing: Energy Reduction Opportunities", Prepared for the DOE-EERE Industrial Technologies Program, (2005).
4. Effectiveness and Impact of Corporate Average Fuel Economy (CAFE) Standards, Transportation Research Board, National Academy Press, (2002).
5. K. Cameron, "Using Ceramics, Brakes Are Light But Cost Is Heavy," The New York Times, June 18, 2006 (2006).
6. G.S. Daehn and M.C. Breslin, "Co-Continuous Composite Materials for Friction and Braking Applications," JOM, November 2006, 89-92 (2006).
7. H. Way, "Media-Milled Nanoparticles Boosts Ceramic Armor," American Ceramic Society Bulletin, Vol 87, No. 5, 20-24, (2008).
8. U.S. Department of Transportation, Research and Innovative Technology Administration, Bureau of Transportation Statistics Report (2005). (http://www.bts.gov/publications/national_transportation_statistics/html/table_01_11.html).
9. D.R. Clarke, "Interpenetrating Phase Composites," Journal of the American Ceramic Society, Vol. 75, No. 4, 739-759, (1992).
10. R. Lenormand and C. Zarcone, "Invasion Percolation in an Etched Network: Measurement of Fractal Dimension," Physics Review Letters, Vol 54, (1985).
11. J.R. Weertman, D. Farkas, K. Hemker, H. Kung, M. Mayo, R. Mitra, and H. Van Swygenhoven, "Structure and Mechanical Behavior of Bulk Nanocrystalline Materials," MRS Bulletin, Vol. 24, No. 2, 44-50 (1999).
12. C.J. Muller, J.M. van Ruitenbeek, and L.J. de Jongh, "Conductance and Supercurrent Discontinuities in Atomic-Scale Metallic Constrictions of Variable Width," Physical Review Letters, Vol. 69, No. 1, 140-143 (1992).
13. L.P. Kouwenhoven and L.C. Venema, "Heat flow through nanobridges," Nature, Vol. 404, 27 April 2000, 943-944 (2000).
14. T.G. Nieh and J. Wadsworth, "Hall-Petch Relation In Nanocrystalline Solids," Scripta Metallurgica, Vol. 25, No. 4, 955-958, (1991).
15. X.F. Zhang, G. Harley, and L.C. De Jonghe, "Co-continuous Metal-Ceramic Nanocomposites," Nano Letters, Vol. 5, No. 6, 1035-1037, (2005).
16. A.S. Zuruzi, M. S. Ward, and N.C. MacDonald, "Fabrication and characterization of patterned micrometre scale interpenetrating Au-TiO₂ network nanocomposites," Nanotechnology, Vol 16, 1029-1034, (2005).
17. J.S. Kim, Y.S. Kwon, O.I. Lomovsky, M.A. Korchagin, V.I. Mali, and D.V. Dudina, "A synthetic route for metal-ceramic interpenetrating phase composites," Materials Letters, Vol. 60, 3723-3726, (2006).

18. C. Badini, M. Pavese, and D. Puppo, "Processing of co-continuous ceramic composites by reactive penetration method: influence of composition of ceramic preforms and infiltrating alloys," *International Journal of Materials and Product Technology*, Vol. 17, No. 3/4, 182-204, (2002).
19. J.D. French, M.P. Harmer, H.M. Chan, and G. A. Miller, "Coarsening-Resistant Dual-Phase Interpenetrating Microstructures," *Journal of the American Ceramic Society*, Vol. 73, No. 8, 2508-2510, (1990).
20. "Block copolymers as templates for functional materials," *Current Opinion in Solid State and Materials Science*, 4, (1999) 587-590.
21. "Identification of the "Voided Double-Gyroid-Channel": A New Morphology in Block Copolymers," *Macromolecules*, 40, (2007) 1066-1072.
22. "Bicontinuous Cubic Morphologies in Block Copolymers and Amphiphile/Water Systems: Mathematical Description through the Minimal Surfaces," *Macromolecules*, 30, (1997) 3395-3402.
23. **Frontiers in transition metal-containing polymer**, by Alaa S. Abd-El-Aziz, Ian Manners, 1st Edition, ISBN-10: 0-471-73015-7, ISBN-13: 978-0-471-73015-6 - John Wiley & Sons, (2007).
24. **Self-assembled nanostructures**, by Jin Z. Zhang, Jun Liu, Shaowei Chen, Gang-Yu Liu, ISBN-0-30647299-6, Kluwer Academic/Plenum Publishers, New York, (2003).
25. "The Plumber's Nightmare: A New Morphology in Block Copolymer-Ceramic Nanocomposites and Mesoporous Aluminosilicates," *J. Am. Chem. Soc.*, 125 (43), (2003) 13084-13093.
26. "Block Copolymer Self-Diffusion in the Gyroid and Cylinder Morphologies," *Macromolecules*, 31, (1998) 5363-5370.
27. "Epitaxial Phase Transformation in Cylindrical and Double Gyroid Mesophases," presented at MRS 2004, (http://www.mrs.org/s_mrs/sec_subscribe.asp?CID=2711&DID=114494&action=detail).
28. "Phase Diagram of Poly(ethylene oxide) and Poly(propylene oxide) Triblock Copolymers in Aqueous Solutions," *Macromolecules*, 39, (2006) 5891-5896.
29. "Structural Study of Mesoporous MCM-48 and Carbon Networks Synthesized in the Spaces of MCM-48 by Electron Crystallography," *J. Phys. Chem. B*, 106, (2002) 1256-1266.
30. "Mesoporous Membrane Templated by a Polymeric Bicontinuous Microemulsion," *Nano Lett.*, 6 (10), (2006) 2354-2357.
31. "Thin Films of Bicontinuous Cubic Mesoporous Silica Templated by a Nonionic Surfactant," *Langmuir*, 20, (2004) 5998-6004.
32. "Nanoprocessing Based on Bicontinuous Microdomains of Block Copolymers: Nanochannels Coated with Metals," *Langmuir*, 13 (26), (1997) pp 6869-6872.
33. "Incorporation of Metal Nanoparticles into a Double Gyroid Network Texture," *Macromolecules*, 39 (21), (2006) 7352-7357.
34. R.S. Addleman, "Nanomaterials for Enhanced Environmental Measurements," Pacific Northwest National Laboratory, Richland, Washington.
35. "Standard Test Method for Flexural Strength of Advanced Ceramics at Ambient Temperature," ASTM C 1161, Annual Book of ASTM Standards Vol. 00.01, American Society for Testing and Materials, West Conshohocken, PA, 2004.
36. TCON Technical Data Sheet, Fireline TCON, Inc., (061018).

37. Information cited from NanoPore website (<http://www.nanopore.com>).

10. Distribution

Internal

1. J.G. Hemrick
2. M.Z. Hu
3. Edgar Lara Curzio
4. Craig Blue
5. Missy Shanken
6. Hiram Rogers

External

7. Klaus-Markus Peters, Fireline TCON, Inc., 300 Andrews Avenue, Youngstown, OH 44505.
8. Brian Hetzel, Fireline, Inc., 300 Andrews Avenue, Youngstown, OH 44505.
9. Joseph Renk, U.S. Department of Energy – National Energy Technology Laboratory, Office of Project Management, 626 Cochran Mill Road, P.O. Box 10940, Pittsburgh, PA 15236.
10. Chien-Wei Li, U.S. Department of Energy – Industrial Technologies Program, Room 5F-065, MS EE-2F, 1000 Independence Avenue, SW, Washington, DC 20585.
11. Ronald Ott, U.S. Department of Energy – Industrial Technologies Program, Room 5F-065, MS EE-2F, 1000 Independence Avenue, SW, Washington, DC 20585.
12. Elmer Fleischman, Idaho National Laboratory, P.O. Box 1625, Idaho Falls, ID 83415.
13. Evgenia Pekarskaya, Lux Research, 140 East 45th Street, 30th Floor, New York, NY 10017.